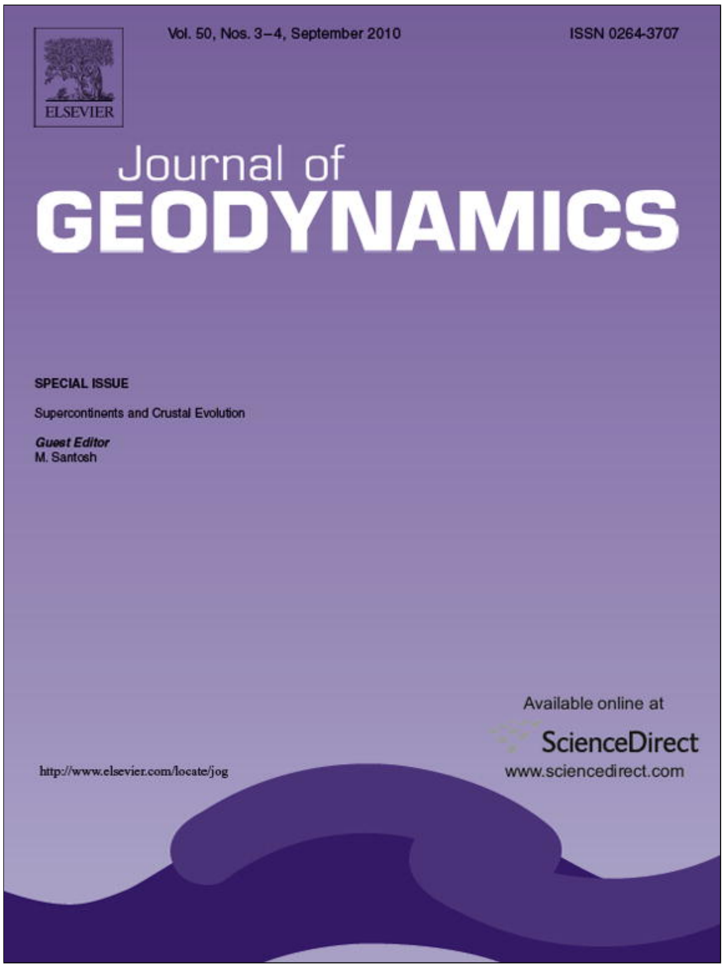
ELSEVIER
Vol. 50, Nos. 3–4, September 2010
ISSN 0264-3707
Journal of
GEODYNAMICS
SPECIAL ISSUE
Supercontinents and Crustal Evolution
Guest Editor
M. Santosh
Available online at
ScienceDirect
www.sciencedirect.com
http://www.elsevier.com/locate/jog

Journal of Geodynamics 50 (2010) 134–153

Contents lists available at ScienceDirect

Journal of Geodynamics

journal homepage: http://www.elsevier.com/locate/jog

LA ICP MS U–Pb ages of detrital zircons from Russia largest rivers: Implications for major granitoid events in Eurasia and global episodes of supercontinent formation

Inna Safonova [a,*], Shige Maruyama [b], Takafumi Hirata [c], Yoshiaki Kon [d], Shuji Rino [b]

[a] Institute of Geology and Mineralogy SB RAS, Koptyuga av. 3, Novosibirsk-90, 630090, Russia
[b] Department of Earth Sciences, Tokyo Institute of Technology, Tokyo 152-8551, Japan
[c] Kyoto University, Oiwakecho, Kitashirakawa, Kyoto 606-8502, Japan
[d] Geological Survey of Japan, AIST, Tsukuba 305-8567, Japan

ARTICLE INFO

Article history:
Received 19 September 2009
Received in revised form 5 February 2010
Accepted 16 February 2010

Keywords:
U–Pb age
Detrital zircon
Peaks of orogeny
Granitoid magmatism
Continental growth
Supercontinents

ABSTRACT

The paper presents LA ICP MS U–Pb age data on detrital zircons from sands of major Russian rivers: the Don, Volga, Ob', Yenisey and Amur. The obtained data are discussed in terms of major episodes of granitic magmatism, which are recorded in the continental blocks that form the modern Eurasian continent. Results are compared with published igneous and detrital zircon age data obtained from parental and sedimentary rocks of the river basins under consideration and worldwide. The U–Pb age results allowed us to confirm (i) the episodic character of continent formation; (ii) the Neoarchean global magmatic event and, possibly, formation of the Kenorland supercontinent; (iii) the global episode of crust formation at 2.0–1.8 Ga, which formed the Columbia supercontinent; (iv) the breakup of Columbia at 1.3–1.2 Ga; (v) the major period of Phanerozoic crustal growth in Central Asia which is likely to be a result of the Altaid orogeny. On the other hand, our data did not unambiguously confirm previous idea about the global character of the Grenvillian and Pan-African orogenies as a result of the assembly of Rodinia and Gondwana, respectively. The "Rodinia" peak is not observed in the histograms of the Ob', Yenisey and Amur, whereas the "Gondwana" signature is not obvious in the histograms of the Don, Volga and Amur. Of special interest are the 2.7–2.5 Ga and 2.0–1.7 Ga peaks in the Ob' zircon age spectrum in spite of the absence of so far identified Archean and Paleoproterozoic parental rocks in the Ob' catchment area. The obtained age spectra were joined into three groups based on statistics: Baltica (Don and Volga), Siberia (Ob' and Yenisey) and East Asia (Amur). For future reconstructions we suggest to include all the available results on Don and Volga rivers into a North America-Baltica Group corresponding to Laurentia-derived continental blocks, and to consider a Siberia Group (Siberian Craton; Ob', Yenisey, Lena, Indigirka rivers) and an East Asia Group (North and South China cratonic blocks; Amur, Yellow, Yangtze and Mekong rivers).

1. Introduction

During recent years the use of detrital zircon data for evaluating the episodic character of crust growth and orogeny, which, to a major extent, is related to global events of granitic magmatism, has become more popular. This can be partly due to the advent of SHRIMP and laser ablation ICP MS U–Pb isotope analysis of zircons, which made the procedure of dating much easier. The recent progress in zircon geochronology and geochemistry (oxygen and Hf isotope and trace element studies) has made a significant impact on our understanding of the crustal evolution of the Earth, thermal history of mountain chains, deep subduction of continental crust, etc. These data corrected the previous curves of continental crust growth (e.g., Dewey and Windley, 1981; Reymer and Schubert, 1984; Armstrong, 1991; McCulloch and Bennet, 1994) and contributed to the estimation of its rate through time. The main benefit from the massive dating of detrital zircons was recognition of the episodic nature of granitic magmatism, which provides a big portion of crust formation, and evaluation of the temporary distribution of granitoid-forming events and the spatial distribution of granitoids complexes (e.g., Condie, 1998; Rino et al., 2004). Detrital zircon U–Pb age populations made it possible to sample indirectly vast segments of continental crust, which are poorly exposed on the surface. Besides, we must take into account that many granitoids dominated crustal terranes could have been eroded away so that evidence for their existence is currently available only in the detri-

* Corresponding author. Tel.: +7 383 335 64 52; fax: +7 383 333 35 84.
E-mail address: inna@uiggm.nsc.ru (I. Safonova).

0264-3707/$ – see front matter © 2010 Elsevier Ltd. All rights reserved.
doi:10.1016/j.jog.2010.02.008

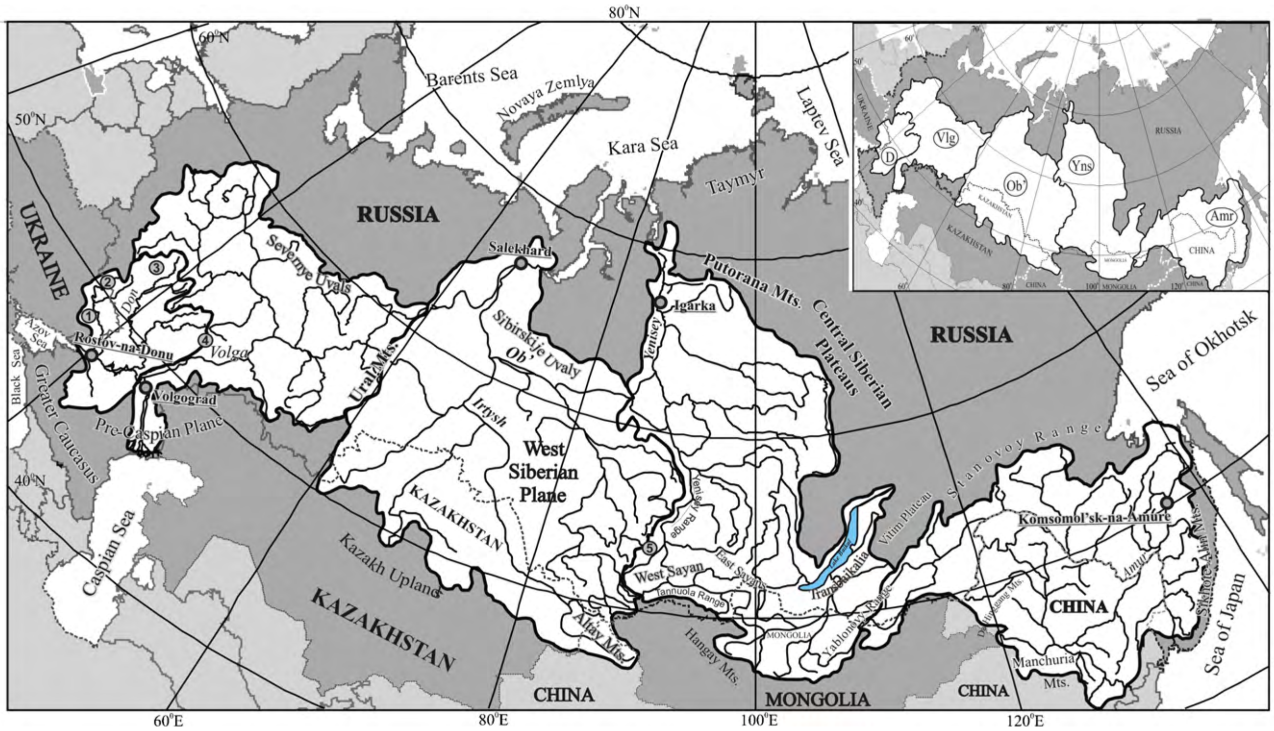

Fig. 1. Geographic outline of drainage areas of Russia major rivers. Fields: white – drainage areas, seas and oceans; grey – countries where not covered by drainage areas. Lines: dashed – state boundaries, black thick – drainage basins, and black thin – river networks. Numbers in circles are other geographic entities: 1 – Don Range, 2 – Middle-Russian (Srednerusskaya) uplift, 3 – Smolensk uplift, 4 – Privolzhskaya uplift, and 5 – Kuznetsk-Alatau Mts.
Letters in circles, in the insert in the right upper corner, indicate relative position of river basins: D – Don, Vg – Volga, Yn – Yenisey, and Am – Amur. River names are shown in italic; sampling locations approximately correspond to those of big cities (see Section 4 for details) which names are underlined.

tal zircon record (Condie et al., 2009). Existing and future scenarios for supercontinent assembly/breakups may benefit from comparison of detrital and granitoid zircon U–Pb age patterns obtained for different present continents.

Recently, the data on detrital zircons from many modern and old world provinces have been obtained and summarized (e.g., Weislogel et al., 2006; Prokopiev et al., 2008; Rino et al., 2008; Condie et al., 2009). However, the main episodes, which have been actively discussed in literature (e.g., Stein and Hofmann, 1994; Condie, 1998), remained those at 2.7 Ga and 1.9 Ga. No notable Phanerozoic peaks have been found for North and South Americas and Africa (Rino et al., 2004, 2008). The detrital zircon data on East Asia showed weak peaks of the Phanerozoic granitic magmatism, however, the amount of the data is rather small and the area so far investigated is restricted by South and North China blocks, i.e., Yellow and Yangtze river basins (Weislogel et al., 2006; Rino et al., 2008; Safonova et al., 2010). Few detrital zircon data have been obtained for Central Asia (namely the Central Asian Orogenic Belt – CAOB), which seems to have significantly contributed to the crustal growth in Asia (Sengör et al., 1993; Jahn et al., 2004). The first data on the Ob' river, which delivers sediments from the northwestern part of the CAOB, were briefly discussed in Rino et al. (2008). The same is true for Europe: only a few works on the detrital zircon geochronology discussing the Volga basin (Allen et al., 2006) and several small rivers in Ukraine (Condie, 2005) are available in the literature.

The period of Late Neoproterozoic-Phanerozoic granitic magmatism is not seen in several published models for crustal evolution based on zircon age peaks (e.g., Condie, 1998; Kemp et al., 2006), but it is quite probable that some previous workers underestimated the amount of Phanerozoic crustal growth/orogenesis because they did not work in Central Asia. Jahn et al. (2000, 2004) and Kovalenko et al. (2004) believe that Central Asia is a region of significant Phanerozoic crustal growth based on abundant geological, age and isotopic data on felsic magmatic rocks from South Siberia, Transbaikalia and Mongolia, however, no age data on detrital zircons from that region have been discussed before.

Thus, the territory of Russia in general and Siberia in particular has long time remained a "blank spot" in terms of detrital zircon geochronology. Rino et al. (2008) presented the first LA ICP MS detrital zircon data on the Ob' river (Fig. 1). This paper presents new LA ICP MS U–Pb ages of detrital zircons from the major rivers of Russia: Don, Volga, Ob', Yenisey and Amur. Besides Russia, the rivers drain adjacent territories of Ukraine, Kazakhstan, China and Mongolia (Fig. 1). The U–Pb age data included in this paper come from the mouths of the Don and Volga rivers in European Russia, and from the Ob', Yenisey and Amur rivers in Asian Russia. The total drainage area of all the river basins under consideration is 9.2 million km^2, i.e., 17% of the area of the whole Eurasian continent. The dataset includes about 2000 ages: about 1500 new original results on the Don, Ob', Yenisey and Amur and 540 results on the Volga and Ob' rivers, which were briefly discussed in Rino et al. (2008). The main goal of the paper is to outline major episodes of granitic magmatism in the continental blocks composing the modern Eurasian continent, to discuss global and local cycles of continental growth and their relation to supercontinent cycles, and to compare our U–Pb results with igneous and detrital zircon age data obtained worldwide. In future these data can be combined with those published by Rino et al. (2004, 2008), Condie (2005) and Condie et al. (2009) to contribute more to our knowledge about the episodic nature of granitic magmatism and the rate of continental growth throughout the Earth's history.

2. Geological review of river basins

Geologically, the territory of Russia consists of two major Archean-Paleoproterozoic cratons of East Europe (East European Craton, EEC, or Baltica or Russian Platform in Russian literature)

Table 1
Main geographic and geological features of the river basins.

River	Catchment area; river length	Discharge sea	Main geological structures within the catchment area	Age of main exposed granitoids[a]	Main references
Don	458,703 km^2; 1950 km	Azov Sea	East European or Baltica Craton (EEC) and its Sarmatia Block; Ukrainian Shield, Voronezh massif, Pripyat-Dniepr-Donetsk rift basin, Donbass coal basin, Karpinskiy Swell, Pre-Caspian Plane, Scythian platform	1. Neoarchean-Paleoproterozoic 2. Early Paleozoic 3. Permian-Triassic 4. Jurassic	Milanovsky et al. (1994), Puchkov (1997, 2003), Glasmacher et al. (2001), Khain and Nikishin (1998), Maystrenko et al. (2003), Bea et al. (2005), Shchipansky et al. (2007), and Bogdanova et al. (2008)
Volga	1,410,994 km^2; 3690 km	Caspian Sea	East European Craton (EEC), Volgo-Uralia Block, Voronezh, Volgo-Uralian and Vyatka massifs, Uralian orogen, Pre-Caspian Plane	1. Archean-Paleoproterozo 2. Meso- and Neoproterozoic 3. Paleozoic	
Ob'	2,972,497 km^2; 5410 km	Kara Sea	West Siberian Basin (WSB), Uralian orogen, Central Asian Orogenic Belt (CAOB): western Altay-Sayan and East Kazakhstan orogens; microcontinents: Kokchetav, Altai-Mongolian and Denisov; Kuzbass coal basin	1. Neoproterozoic 2. Paleozoic 3. Early Mesozoic	Vladimirov et al. (1997, 1998, 1999), Rosen et al. (1994), Fershtater et al. (1997), Kruk et al. (1999), Nozhkin et al. (1999), Heinhorst et al. (2000), Buslov et al. (2001), Yarmolyuk et al. (2001), Hong et al. (2004), and Turkina et al. (2007)
Yenisey	2,554,482 km^2; 4012 km	Kara Sea	Siberian Craton; Permo-Triassic flood basalts, Tunguska, Altai-Mongolian and Tuva-Mongolian microcontinents/terranes; CAOB: eastern Altay-Sayan, Hingai and Transbaikalia orogens	1. Archean-Paleoproterozoic 2. Late Neoproterozoic-Phanerozoic	
Amur	2,824,000 km^2; 4440 km	Sea of Okhotsk	Siberian and North China Cratons; Tuva-Mongolian, Argun-Indermeg and Bureya-Jiamusi microcontinents; Umlekan-Ogodzhin, Uda-Stanovoy, Mongol-Okhotsk and Sikhote-Alin orogenic belts	1. Archean-Paleoproterozoic 2. Late Paleozoic-Early Mesozoic 3. Late Mesozoic-Cenozoic	Sakhno (2001), Kovalenko et al. (2004), Karsakov et al. (2005), and Parfenov et al. (2006)

[a] Detailed description of geological features of river basins and their ages is given in Sections 2 and 4.

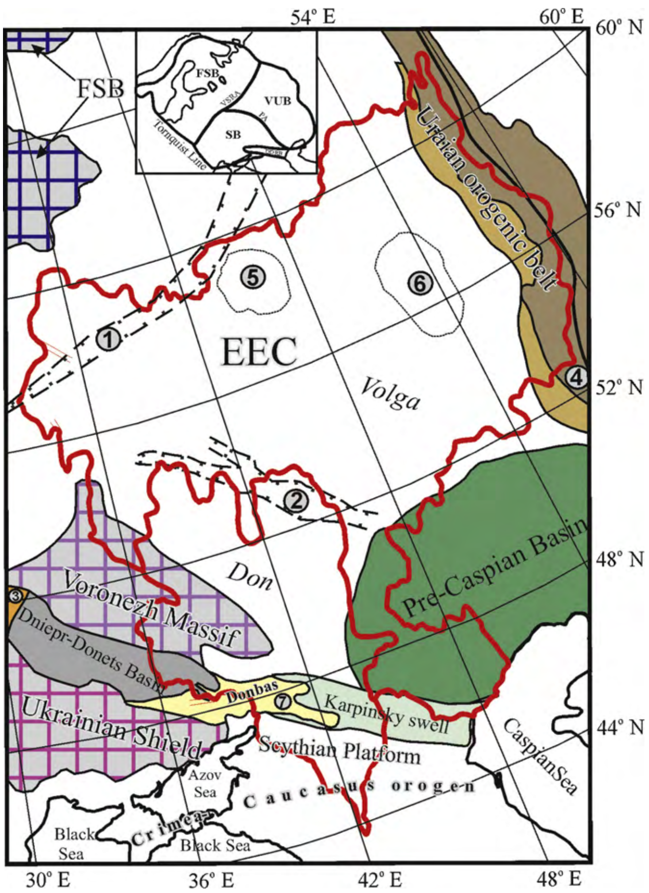

Fig. 2. Geological scheme of the Don–Volga drainage area (solid bold line) and adjacent territory. The index insert map shows main elements of the East European Craton (EEC): FSB – Fennoscandia block, SB – Sarmatia block, VUB – Volgo-Uralia block. Numbers in circles: 1 and 2 – aulacogenes (1 – Volyn'-Srednerusskiy, 2 – Pachelma); 3 – Pripyat trough, 4 – Uralian Main Granite Axis; 5 and 6 – buried massifs (5 – Vyatka, 6 – Volgo-Uralian); 7 – Donetsk foldbelt.

and Siberia (Siberian Platform or Craton), large swathes of the Altaids/CAOB and a complex segment of Russian Far East consisting of geological units of different geodynamic origin (Zonenshain et al., 1990). The East European and Siberian Cratons are separated by the Ural Mountains and the world famous West Siberian Basin (WSB), which hosts rich oil and gas deposits (Fig. 1). European Russia consists of three Late Archaean-Early Proterozoic cratonic blocks of the EEC, Fennoscandia, Sarmatia and Volgo-Uralia (Fig. 2; Bogdanova, 1993). The EEC is bounded in the east by the Uralian and Novaya Zemlya orogens, to the south by the Scythian Platform and Crimea-Caucasus orogen, to the southwest by the Tornquist Line, to the northwest by the Scandinavian Caledonides and to the north by Arctic oceanic realms (Nikishin et al., 1996; Fig. 2). The Siberian Craton is bounded in the east by the Verkhoyansk orogen, to the south by the CAOB including Altay-Sayan, Yenisey-Transbaikalian, and Stanovoy orogens, to the west by the East Angara and Yenisey Range orogens and to the north by the Southern Taymyr orogen (Karsakov et al., 2005; Smelov and Timofeev, 2007; Figs. 3–5). The geological structure of Russian Far East includes numerous foldbelts, continental blocks, continental margin (passive and active), island/back/fore-arc, accretionary and oceanic terranes (Fig. 5; Zonenshain et al., 1990; Karsakov et al., 2005).

The Volga and Don rivers deliver sediments mainly from the EEC (territories of Ukraine and Russia); the Ob' river – from the WSB and its bounding orogenic belts of the Urals, Altai-Sayan and North-East Kazakhstan (territories of Russia, Kazakhstan, Mongolia and China); the Yenisey river – from the Siberian Platform and its mountain frame of the Yenisey Range, East and West Sayan and Transbaikalia (Russia and Mongolia), and the Amur river – from the Argun-Indermeg and Bureya-Jiamusi continental blocks, Stanovoy and Mongol-Okhotsk orogens and tectonic collages of Proterozoic to Cenozoic island-arc, continental margin arc, passive margin and accretionary terranes (territories of Russia, China and Mongolia; Figs. 1–5). Due to the thick Mesozoic-Cenozoic covers on the low lands, and because of the extensively developed Phanerozoic tectonically controlled basins, the basement geology of all the rivers in general, and of the Volga, Yenisey and Ob' basins in particular has not been well investigated. Table 1 shows general geographic and geological information about the river catchment areas under consideration.

2.1. The Don

The Don drains an area of ca. 0.42 million km^2 (Table 1). The Don drainage basin or catchment area[1] extends from the Donetsk Range and Middle-Russian (Srednerusskaya) uplift on the west, Smolensk uplift in the north, Privolzhskaya uplift on the east, and the Pre-Caspian Plain and the Greater Caucasus (Crimea-Caucasus) on the southeast and south, respectively (Fig. 1). Geologically, the Don drainage basin includes the Precambrian Voronezh Massif, the Devonian NW-SE striking Pripyat-Dniepr-Donetsk rift basin, and the Paleozoic Scythian Platform (Fig. 2). The Voronezh Massif, along with the well-known Ukrainian Shield, is an exposed part of the Sarmatia cratonic block of Archean-Paleoproterozoic age, which is a segment of the EEC (Shchipansky and Bogdanova, 1996; Shchipansky et al., 2007). The Pripyat-Dniepr-Donetsk basin consists of the shallower Pripyat trough (northwest), the deeper Dniepr-Donetsk basin including the Donbass coal-bearing basin (central part) and the uplifted Donbass foldbelt and Karpinsky swell (southeast; Maystrenko et al., 2003). In general, the bedrock of the Don catchment consists of Paleozoic and Mesozoic sediments uncomfortably overlying Precambrian crystalline rocks. Locally, the sediments are intruded by Late Devonian, Permian-Triassic and Jurassic magmatic rocks (Nalivkin, 1983; Wilson and Lyashkevich, 1996). The basement is dominated by the Sarmatia block and includes small segments of the Volgo-Uralia block in the northeast and of the Scythian Platform in the southeast (Fig. 2).

2.2. The Volga

The Volga delivers sediment from a drainage area ca. 1.4 million km^2 (Table 1; Fig. 1), which neighbors the Don basin from the east. The Volga catchment is bounded by the Privolzhskaya Uplift in the west, Severnye Uvals to the north, Ural Mountains to the east and Pre-Caspian Plain in the south (Fig. 1). Most of the catchment lies within the Volgo-Uralia block and from the southwest it is bounded by the Pachelma aulacogen. The bedrock of the Volga catchment area is dominated by Phanerozoic sediments that form the cover of the EEC. The basement of the Volga catchment includes units of the EEC and the folded units of the Uralian orogen bounding the EEC to the east. The EEC is exposed in the Voronezh Massif (in the southwest), a part of the former Sarmatia block, and in the Volgo-Uralian and Vyatka Massifs, buried parts of the former Volgo-Uralia block (Khain and Nikishin, 1998). There are also exposures of Precambrian rocks in this region along the western side of the Urals (Puchkov, 1997) showing evidence for both Meso- and Neoproterozoic orogeny (Glasmacher et al., 2001). Phanerozoic sediments deposited across the craton are presumably derived

[1] Drainage basin, drainage area, catchment area or simply basin or catchment—in this paper all these terms are equivalently used to define an area, which a river with all its tributaries can deliver sediments from.

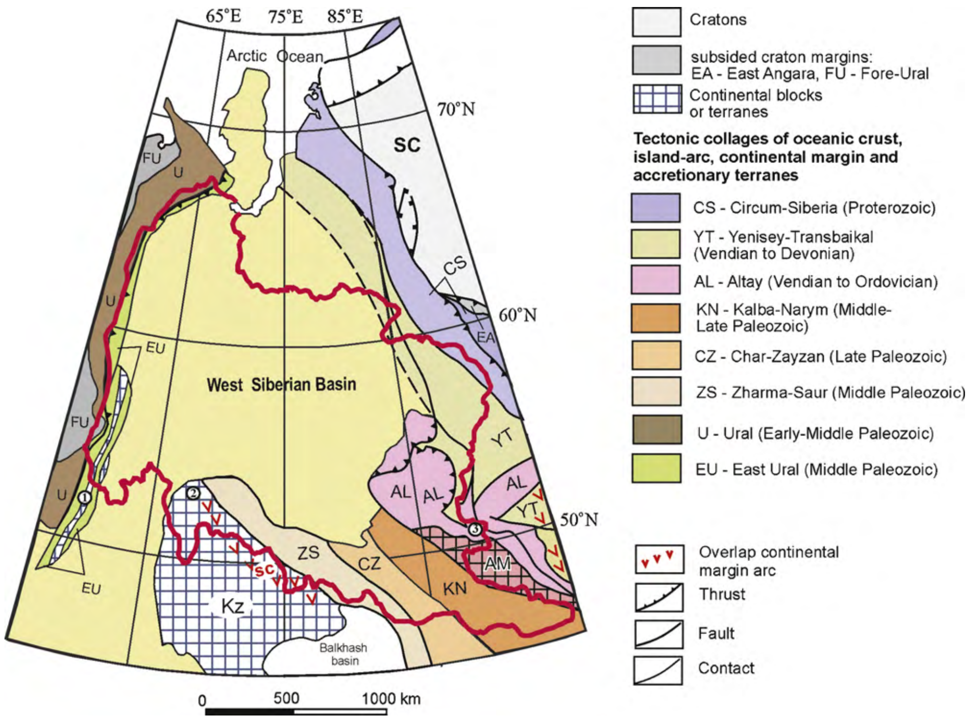

Fig. 3. Geological scheme of the Ob' drainage area and adjacent territory (modified from Nalivkin, 1983; Parfenov et al., 2006). *Abbreviations*: SC – Siberian Craton, Kz – Kazakhstan continental block (Archean-Proterozoic?), AM – Altay-Mongolian microcontinent or superterrane; sc – Stepnyak-Chingiz (Early-Middle Paleozoic) overlap continental margin arcs. Numbers in circles are for exposed Precambrian terranes: 1 – Denisov, 2 – Kokchetav, and 3 – Gornaya Shoriya. The thick red line outlines the drainage basin. (For interpretation of the references to color in this figure legend, the reader is referred to the web version of the article.)

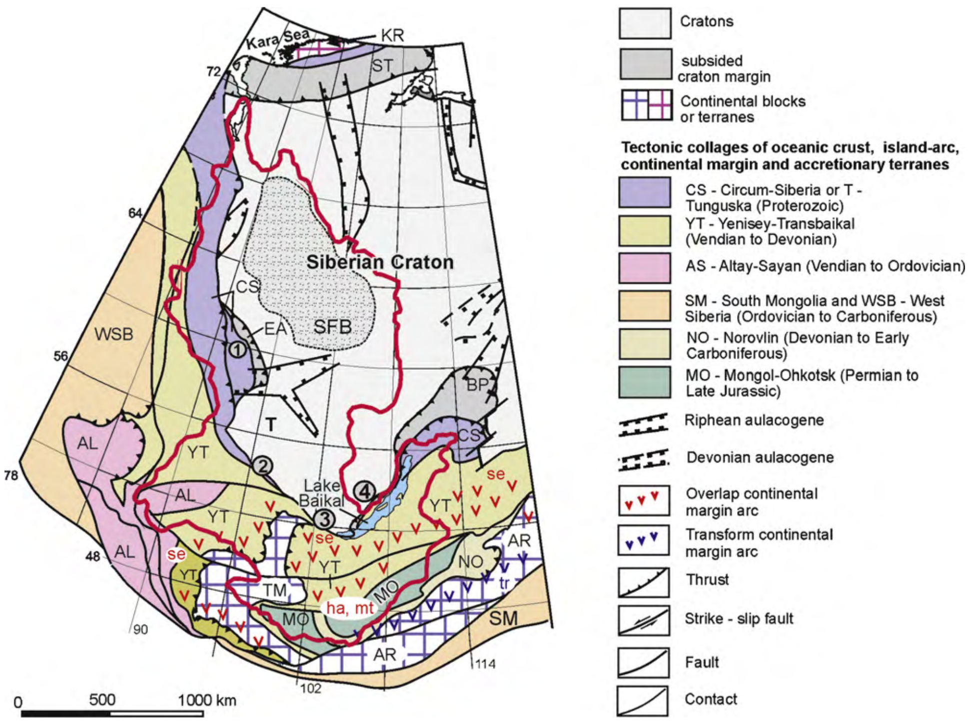

Fig. 4. Geological scheme of the Yenisey drainage area and adjacent territory (modified from Parfenov et al., 2006). *Superterranes*: AR – Argun-Idermeg (Proterozoic to Devonian); BP – Baikal-Patom (Riphean to Cambrian and older basement); EA – East Angara (Riphean and older basement); KR – Kara (Proterozoic to Permian); ST – South Taimyr (Ordovician to Jurassic); T – Tunguska, buried (Archean-Paleoproterozoic); TM – Tuva-Mongolian (Proterozoic to Devonian). *Overlap continental margin arcs* (younger to older): ha – Hangay (Late Carboniferous to Early Permian, 320–272 Ma), mt – Mongol-Transbaikalia (Late Triassic to Early Cretaceous, 230–96 Ma), se – Selenga (Permian to Jurassic, 295–135 Ma); tr – Trans-Baikalian arc formed along intraplate strike-slip fault (Middle Jurassic–Early Cretaceous, 175–96 Ma). WSB – West Siberian Basin; SFB – Siberian Flood Basalts. Numbers in circles (exposed Precambrian terranes): 1 – Angara-Kan, 2 – Biryusa, 3 – Sharyzhalgai, and 4 – Akitkan. The thick red line outlines the drainage basin. (For interpretation of the references to color in this figure legend, the reader is referred to the web version of the article.)

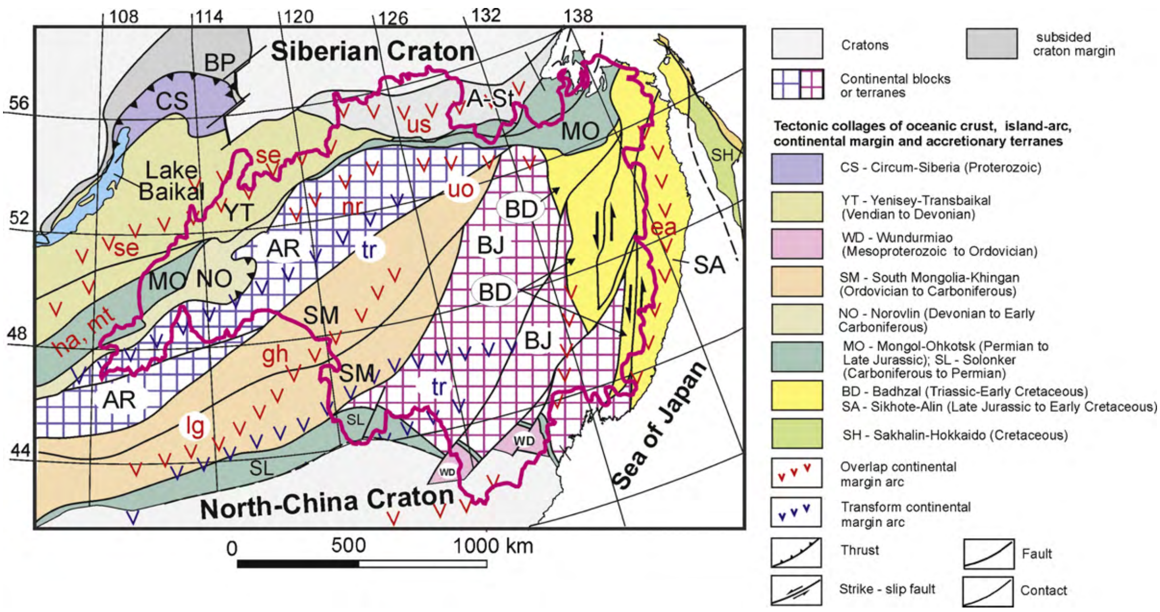

Fig. 5. Geological scheme of the Amur drainage area and adjacent territory (modified from Parfenov et al., 2006). *Continental blocks or superterranes*: AR – Argun-Idermeg (Proterozoic to Devonian); BJ – Bureya-Jiamusi (Archean to Permian); Subsided craton margins: BP – Baikal-Patom (Riphean to Cambrian and older basement), A-Se – Aldan-Stanovoy (Archean-Paleoproterozoic). *Overlap continental margin arcs* (younger to older): ea – East Sikhote-Alin (Late Cretaceous to early Tertiary, 96–65 Ma), ha – Hangay (Late Carboniferous to Early Permian, 320–272 Ma), gh – Gobi-Hangay (Permian, 295–250 Ma), lg – Lugyngol (Permian, 295–250 Ma), mt – Mongol-Transbaikalia (Late Triassic to Early Cretaceous, 230–96 Ma), se – Selenga (Permian to Jurassic, 295–135 Ma), sm – South Mongolian (Middle Carboniferous through Triassic, 320–203 Ma), uo – Umlekan-Ogodzhin (Cretaceous, 135–65 Ma), us – Uda-Stanovoy (Jurassic to Early Cretaceous, 203–96 Ma), tr – Trans-Baikalian arc formed along intraplate strike-slip fault (Middle Jurassic–Early Cretaceous, 175–96 Ma). The thick red line outlines the drainage basin. (For interpretation of the references to color in this figure legend, the reader is referred to the web version of the article.)

from a combination of the Precambrian basement blocks and the Paleozoic Uralian orogenic belt. Besides, the catchment includes a small part of the Karpinsky Swell to the south (Fig. 2).

2.3. The Ob'

The Ob' river delivers sediment from a drainage area ca. 2.9 million km^2 (Table 1). The Ob' catchment area is adjacent to the Volga basin in the west and 70% of it consists of the West Siberian Basin (WSB) surrounded by the Ural Mountains, Kazakh Uplands, Altay, West Sayan and Kuznetsk Alatau Mts. and Sibirskije Uvaly or Uplift (from west to east, counter clockwise; Fig. 1). The WSB is dominated by Meso-Cenozoic sediments several kilometers thick and is framed by the Uralian orogen to the west, the CAOB and Kokchetav continental block (or microcontinent) to the south, and the Kuzbass coal-bearing basin to the southeast (Fig. 3). Thus, the catchment includes the Denisov (southern Urals), Kokchetav (northern Kazakhstan) and Altai-Mongolian (Russian and Mongolian Altay) terranes/microcontinents, Uralian orogen and CAOB including East Kazakhstan and Altai-Sayan folded structures (Table 1; Buslov et al., 2001; Puchkov, 2003; Samygin and Burtman, 2009). In the east the Ob' basin is separated from the Siberian Craton by the Yenisey fault, therefore the Proterozoic Yenisey Ridge is located beyond the bounds of the Ob' catchment. The bedrock of the catchment area consists of typical Late Neoproterozoic-Paleozoic foldbelts of the CAOB, which comprise diverse oceanic and island-arc units, anorogenic and post-orogenic granites (Buslov et al., 2001, 2004a; Kovalenko et al., 2004). In general, the CAOB formed due to Late Neoproterozoic-Early Paleozoic subduction and Middle-Late Paleozoic closure of the Paleo-Asian Ocean (Dobretsov et al., 1995; Buslov et al., 2001) accompanied by several stages of continental collision of large continental blocks and Gondwana-derived terranes or microcontinents: the Early Paleozoic collision of the Siberian continent and Altai-Mongolian microcontinent, the Late Paleozoic collision of the Siberian and Kazakhstan continents, and the Cenozoic collision of the Indo-Australian Plate and Eurasian continent (e.g., Buslov et al., 2001, 2004a; Molnar and Tapponnier, 1975). The Uralian orogen was formed during the Late Paleozoic collision of Kazakhstan, Baltica and Siberia (Puchkov, 1997).

2.4. The Yenisey

The Yenisey river has a drainage area ca. 2.6 million km^2 (Table 1). The Yenisey catchment area borders the Ob' catchment in the west and occupies the western part of East Siberia (Siberian Craton/Platform; Fig. 1). It is bounded by the Putorana Mountains (plateau) to the north, Central Siberian plateaus in the east, Yablonovyy Range in the southeast, Hingai (Hangayn) Mountains to the south, Tannuola Range to the southwest, and the Kuznetsk Alatau Mountains and the Yenisey Ridge to the west (Fig. 1). The Yenisey drainage basin separates the Ob' drainage basin from the Yenisey Ridge. Most of the Yenisey bedrock consists of Phanerozoic sediments and Permo-Triassic Siberian Flood Basalts (Siberian Traps) forming the cover to the Siberian Craton, Late Neoproterozoic-Phanerozoic units of the CAOB (East and West Sayans) and the Late Neoproterozoic Yenisey-Transbaikalian orogen (Fig. 4). The basement consists of Precambrian continental blocks (e.g., Baikal-Patom, Tunguska and Tuva-Mongolian) and Neoproterozoic-Early Paleozoic foldbelts that outcrop by the periphery of the platform cover. Although the Siberian Traps occupy about 25% of the area, this province made no essential contribution to the age population of zircons due to the scarcity of zircon in mafic rocks. The platform sediments and flood basalts cover the Tunguska block, which occupies the western part of the catchment and is exposed in the Kan and Sharyzhalgai terranes including Archean granulite-gneisses and greenstones and Paleoproterozoic collisional granites (Aftalion et al., 1991; Rosen et al., 1994). From the west and southwest the Tunguska block is bounded by the Circum-Siberia foldbelt built over an Archean-Proterozoic basement (Rosen et al., 1993; Nozhkin et al., 1999). The eastern part of the catchment includes the Akitkan or Baikal uplift of the Baikal-Patom margin fringing the Siberian Craton along the northern shore of Lake Baikal (Fig. 4; Parfenov et al., 2006; Smelov and Timofeev, 2007).

2.5. The Amur

The Amur basin has a relatively short common border with the Yenisey basin at its western part (Figs. 1, 4 and 5). The Amur delivers sediment from a drainage area ca. 1.9 million km^2 (Table 1). The catchment has a complicated structure because it includes the junction zone between the Siberian and North China Cratons. In the north it is bounded by the Stanovoy Range, Sikhote-Alin Mountains to the east, Hangay (Da Hinggang) and Manchuria Mountains to the south and Yablonovy Range to the west (Fig. 1). The Amur bedrock is dominated by Archean crystalline blocks of Siberia (Stanovoy granite-greenstone belt) and North China (Umlekan-Ogodzhin belt) and orogenic structures of the Stanovoy (Proterozoic), Mongol-Okhotsk (Late Paleozoic-Mesozoic) and Sikhote-Alin (Late Mesozoic) foldbelts. It also includes the East Sikhote-Alin active continental margin volcanic belt (Late Mesozoic-Cenozoic), which hosts Permian-Triassic and Jurassic accretionary prisms. There are also Archean-Proterozoic Bureya-Jiamusi (east) and Proterozoic Argun-Indermeg (west) continental blocks "rejuvenated" by numerous Paleozoic granitic intrusions (Fig. 5). The widely exposed basement and orogenic units locally are covered by Mesozoic and Cenozoic superimposed basins (Zonenshain et al., 1990; Karsakov et al., 2005; Parfenov et al., 2006). However, the area of superimposed basins within the Amur catchment is much smaller than that of the Ob' and Yenisey basins, therefore its is easier to correlate the basement geology and the U–Pb age peaks.

3. Methods and approaches

In this section we discuss the methods of sample preparation and isotope analysis as well as our approaches in processing of analytical data and their interpretation. Generally, we assume that the U–Pb system in zircons is very stable, and is weakly affected by post-magmatic processes of sedimentation or metamorphism (up to the middle amphibolite facies). Consequently, the LA ICP MS age of a detrital zircon represents the original crystallization age; however this does not mean that the zircon was derived directly from basement of that age, because it could have been recycled many times. We accept that the vast majority of zircons are of intermediate–acidic igneous parentage (Deer et al., 1997), although they do also occur rarely in basic igneous rocks.

3.1. Zircon sample preparation

Zircons were randomly handpicked from the non-electromagnetic heavy mineral separates prepared in the IGM SB RAS, then mounted and polished. In order to avoid or at least minimize potential biasing of age data at least two grain mounts covering a range of zircon sizes were prepared for each sample. More subjectivity in zircon dating was avoided by analyzing all zircons encountered during the traverse of the mount, unless the grain showed evidence of being metamictic and/or otherwise structurally changed. Zircons affected by metamorphic processes such as those with homogenous texture, overgrowths or rims/mantles, etc. were excluded as well. Most zircons are colorless or light-colored, subhedral to euhedral in shape and 50–150 μm in size and display oscillatory zoning patterns indicative of their magmatic origin. All these determinations were made

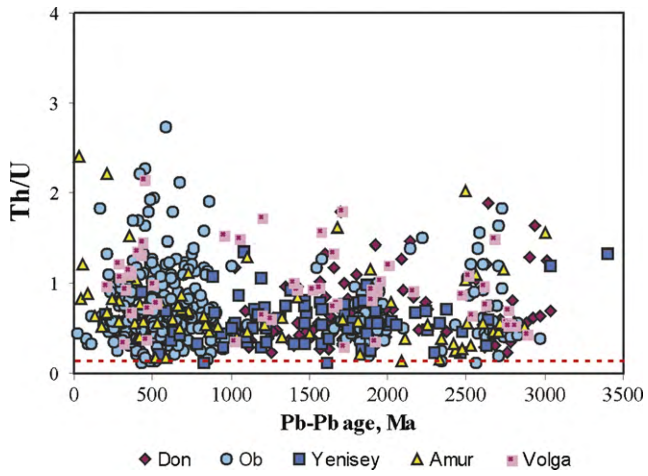

Fig. 6. Pb-Pb ages versus Th/U ratios in detrital zircons from sand of the Don, Volga, Ob', Yenisey and Amur rivers. The red dashed line marks the 0.1 Th/U level. (For interpretation of the references to color in this figure legend, the reader is referred to the web version of the article.)

from examination of the reflected- and transmitted-light photomicrographs and cathode luminescence (CL) images. The ages reported from zircon chronology in this paper are from the cores of igneous/zoned zircons. More control for the magmatic origin of the zircons selected for geochronology was made by checking their Th/U ratio (Fig. 6), which is expected to be higher than 0.1 but less than 1.0 in igneous zircons (Whitehouse et al., 1999; Hoskin and Black, 2000). The absence of Th/U correlation with age values also suggests their magmatic origin (Fig. 6). Due to careful hand-picking, optical and chemical control the metamorphic zircons appeared to constitute less than 1% of more than 2000 zircon grains studied. Thus, our choice of magmatic zircons was based on oscillatory zoning patterns, 2 > Th/U > 0.1 and absence of Th/U correlation with age values.

3.2. Age dating analytical procedures

The spot analysis of detrital zircons was performed with a ThermoElemental VG PlasmaQuad 2 ICP MS (see Rino et al., 2004 for details) in the Tokyo Institute of Technology (Titech). The zircons from the Volga and Ob' rivers were analyzed using a MicroLas GeoLas 200CQ laser ablation system equipped with a Lambda Physik COMPex 102 ArF excimer laser as a 193 nm DUV (deep ultraviolet) light source. The instrumental sensitivities achieved by the LA ICP MS are 1.5×10^4 cps/μg g^{-1} for Pb and U on NIST 610 SRM from a diameter of 20 μm spot size ablated by a 5 Hz repetition rate with a source pulse energy of 140 mJ. The zircons from the Don, Yenisey and Amur rivers were analyzed using a S-option interface (Hirata and Nesbitt, 1995; Hirata, 2000) and an in-house laser ablation system based on a 230 fs titanium-sapphire regenerative amplifier system (IFRIT, Cyber Laser, Titech, Japan) operating at a fundamental wavelength of 780 ± 20 nm (near infrared red, NIR). In that case, He gas instead of Ar gas was used as a carrier gas, which improved the sample transport efficiency from the sample cell to the ICP, and reduced sample deposition around the ablation pit (Eggins et al., 1998). Operational settings such as ICP conditions and lens biases were optimized to maximize the signal intensity of the ^{208}Pb signal obtained by laser ablation of NIST SRM610. The ion sampling depth and ion energy were carefully optimized to maximize the signal intensity and to minimize the background count at ^{208} Dalton. All measurements were carried out with peak jump acquisition mode at the peaks ^{139}La, ^{202}Hg, ^{204}Pb (^{204}Hg), ^{206}Pb, ^{207}Pb, ^{232}Th and ^{238}U. A major problem associated with the analysis of ^{204}Pb using the LA

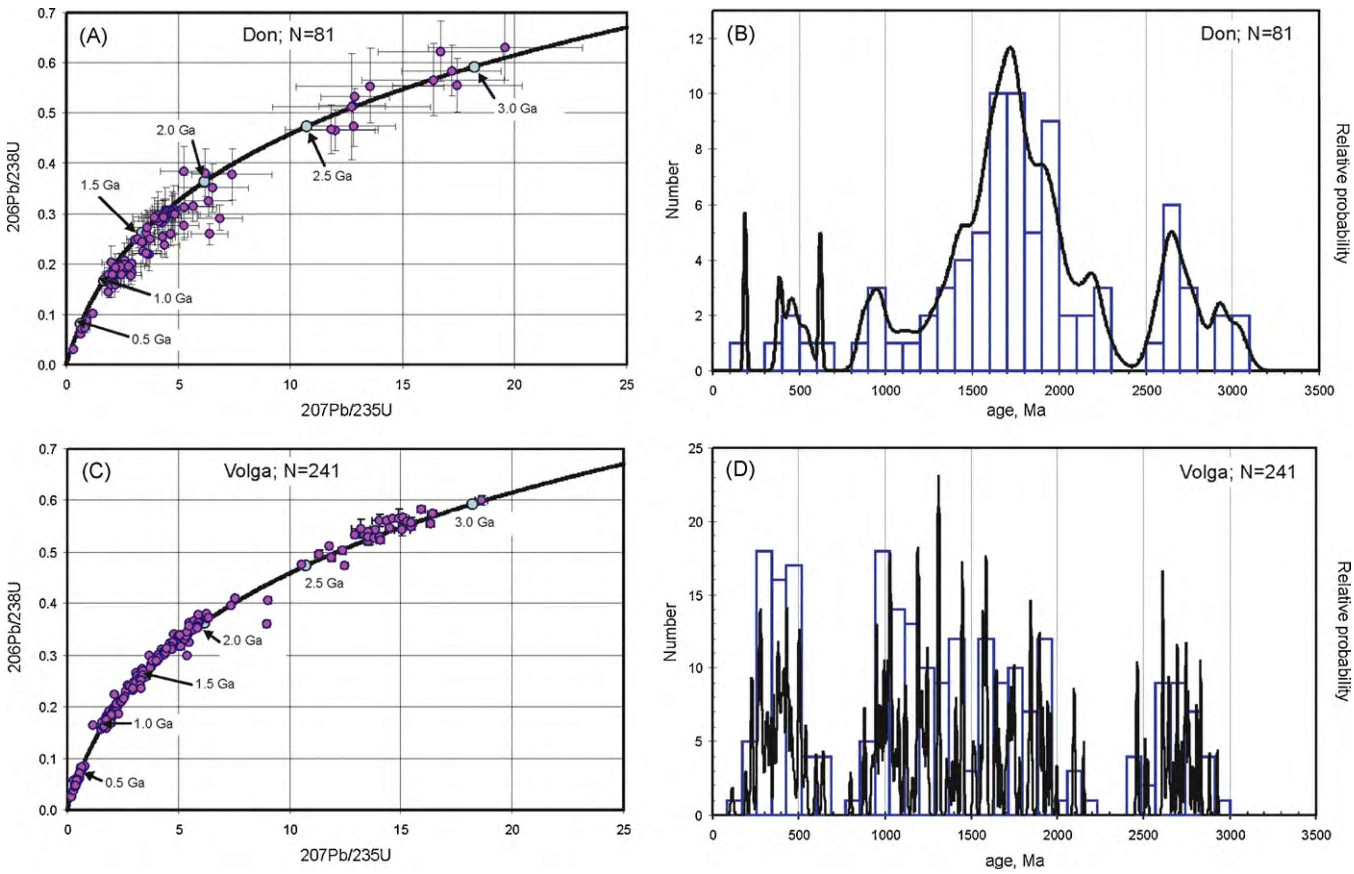

Fig. 7. U–Pb concordia diagrams (left) and age histograms (right) coupled with probability density distribution (PDD) plots for in-site analyses of detrital zircons from the Don (a, b) and Volga (b, c) river mouth sand. The error bar is two sigma.

ICP MS is ^{204}Hg isobaric interference. The ^{204}Hg mainly originates from Ar gas, since the Hg signals do not decay with time. ^{204}Hg was corrected by measuring ^{202}Hg. In order to reduce the isobaric interference of ^{204}Hg, a Hg-trap device using an activated charcoal filter was applied to the Ar make-up gas before mixing with He carrier gas (Hirata et al., 2005).

3.3. Data processing

The U–Pb results are displayed in concordia diagrams and age spectra/histograms with their associated probability density distribution (PDD) plots (Figs. 7–9). For all groups of data most of grains plot on the single stage Pb isotope evolution curve, i.e., concordia, within analytical error and give the ages to be discussed below. The rest of the grains plot off the curve, i.e., concordia. We could not obtain true discordant ages for the grains plotted off the curve, because they obviously have different origin, i.e., we do not know which magmatic massifs they came from and when was the event which resulted in Pb loss. Therefore, we calculated ^{207}Pb/^{206}Pb ages for the discordant U–Pb (^{206}Pb/^{238}U and ^{207}Pb/^{235}U) ages. The grains on the curve have the same U–Pb and Pb–Pb radiogenic ages and those plotted off the curve have minimal Pb–Pb ages. In case of possible common-Pb contamination, which increases Pb/U ratio especially for ^{207}Pb/^{235}U, and at low signal intensity the ^{206}Pb/^{238}U ages seem to be reliable due to much higher signal intensities of ^{206}Pb compared to those of ^{207}Pb. The details of the technique of common-Pb correction are given in Hirata and Nesbitt (1995). Therefore, for constructing histograms and PDD plots we used ^{206}Pb/^{238}U results for the ages younger than 1 Ga and ^{207}Pb/^{206}Pb results for the ages older than 1 Ga, which are consistent independently of the type of laser device used for the dating. The percentages of different age groups recognized within each river basin are listed in Table 2. In order to estimate proportions of Phanerozoic, Proterozoic and Archean grains in the samples with the introduction of least possible bias, discordant analyses were used in all calculations where possible. The portion of discordant grains ranges from 1 to 5% in the Volga and Ob' samples analyzed with the excimer laser to 30–40% in the Don, Yenisey and Amur samples analyzed with the femtosecond laser. The data with concordance <95% obtained at low signal intensity (^{207}Pb background intensity) and the low concordant data (<70%) obtained at sufficient signal intensity were excluded from the final datasets of the Don, Yenisey and Amur used for constructing the histograms (Figs. 7b, d, 8b, d, 9b, and 10).

The age histograms with probability density curves were generated using ISOPLOT (Ludwig, 1999). Representative analytical data on zircons from the river mouths under consideration are given in Appendix A supplementary electronic data table. All the age data were also processed with statistical methods (see Section 5.5).

Table 2
Percentage of U–Pb zircon ages for each river catchment.

Era, river	Don	Volga	Ob'	Yenisey	Amur
Cenozoic (0–65 Ma)	0	0	0	0	0
Mesozoic (65–250 Ma)	1	2	7	5	**48**
Paleozoic (250–542 Ma)	5	**22**	**43**	**54**	17
Neoproterozoic (542–1000 Ma)	6	10	18	14	1
Mesoproterozoic (1000–1600 Ma)	**21**	**32**	2	1	1
Paleoproterozoic (1600–2500 Ma)	**49**	19	**19**	**20**	**23**
Neoarchean (2500–2800 Ma)	12	10	10	4	10
Mesoarchean (2800–3200 Ma)	5	3	1	1	1

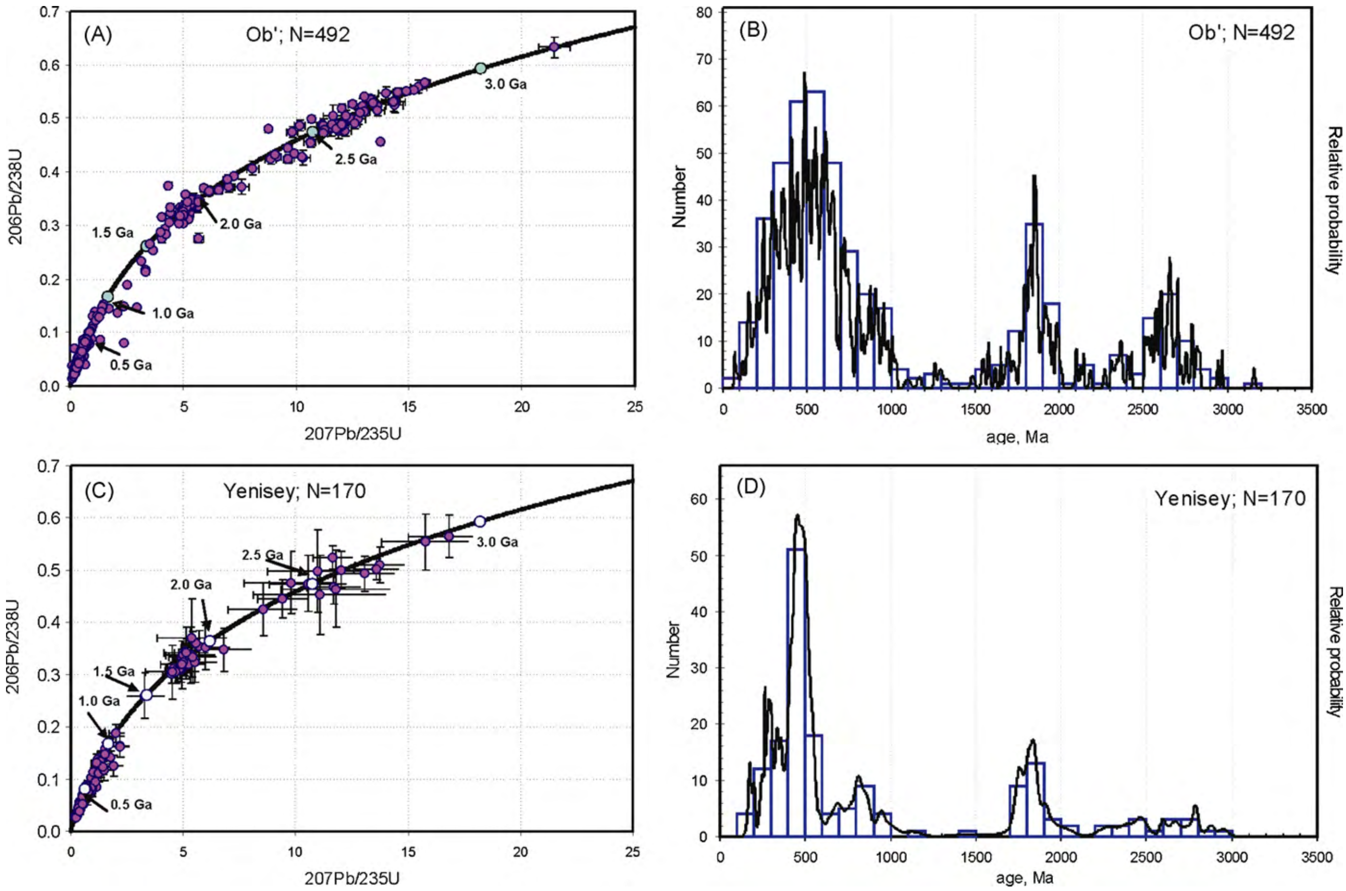

Fig. 8. U–Pb concordia diagrams (left) and age histograms (right) coupled with PDD plots for in-site analyses of detrital zircons from the Ob' (a, b) and Yenisey (c, d) river mouth sand. The error bar is two sigma.

3.4. Correlation of basement geology and zircon ages

While interpreting the peaks on detrital zircon age spectra/histograms we must access the involvement of basement rocks buried beneath superimposed sedimentary and volcanic covers and to which degree the proportions of the zircon age peaks depend on drainage area topography and distance from headwaters. If the basement is covered by sedimentary rocks it is quite probable that the natural processes of sediment erosion provide homogeneous mixing rather than heterogeneous differentiation (Rino et al., 2008). In case of volcanic covers typically consisting of mafic flows, e.g., the Yenisey drainage basin is 25% covered by the Siberian flood basalts, we suggest that zircons from the basement are hardly involved in transportation by streams. Therefore, in those cases, we must be careful while comparing the areas of exposed rocks of a certain age with the percentage of peaks in age histograms, and the volcanic-covered areas should be excluded from consideration.

On the other hand, we believe that the transportation of zircons of 50–200 μm in size minimally, if at all, depends on the topography and the distance from source. If we accept that rivers derive a disproportional fraction of their load from rapidly eroding, i.e., usually young orogenic areas, then the zircon dataset must be over-

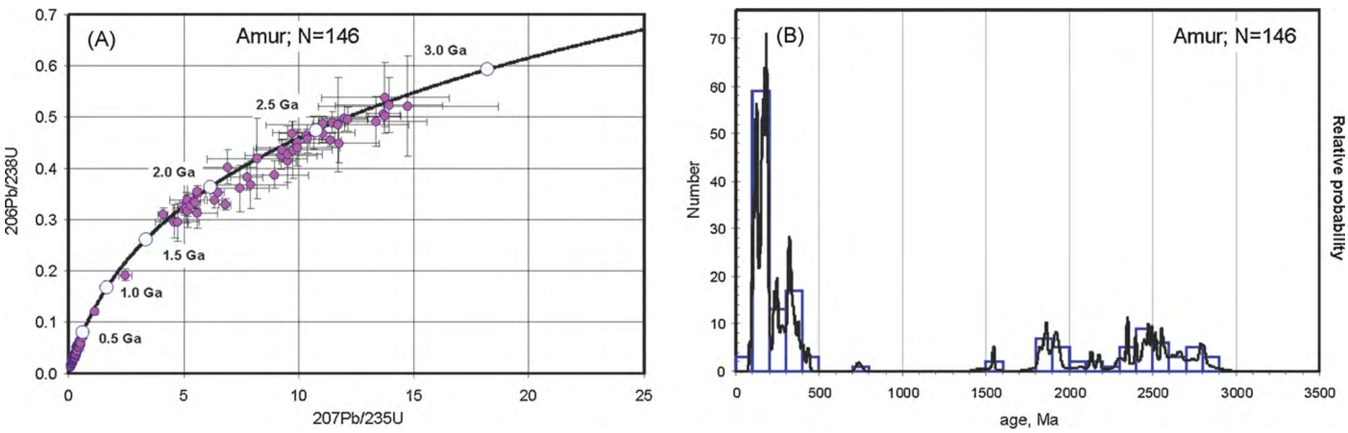

Fig. 9. U–Pb concordia diagrams (a) and age histograms (b) coupled with PDD plots for in-site analyses of detrital zircons from the Amur river mouth sand. The error bar is two sigma.

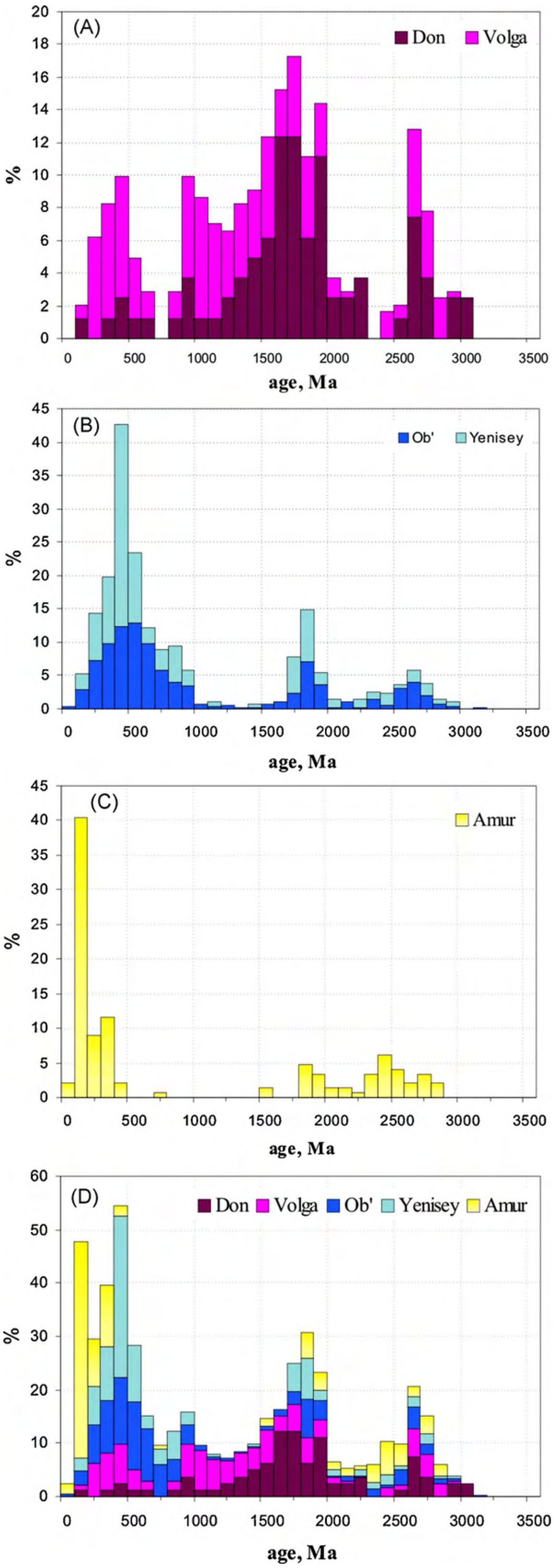

Fig. 10. Frequency distribution cumulative histograms normalized to 100% for three groups documented by major river mouth zircons. "Baltica" Group 1 (a) is from the EEC and Uralian orogen (the Don and Volga); "Siberia" Group 2 (b) includes the Siberian Craton, Kazakhstan continental block, Central Asian and Uralian orogens (the Ob' and Yenisey); "Far East" Group 3 (c) includes the Siberian and North China Cratons and Pacific margin orogen (the Amur). Note the absence of Pan-African zircons in the "Baltica" and "Far East" Groups and the absence of Grenvillian zircons in the "Siberia" and "Far East" Groups. The total histogram (d) shows four evident peaks at 2.8–2.6 Ga, 2.0–1.8 Ga, 0.5–0.4 Ga and 0.2–0.1 Ga.

saturated by younger grains. In that case we must expect that the Volga zircon population will be dominated by the Paleozoic ages of the North and Middle Urals, because the areas providing Precambrian zircons, namely the Voronezh Massif and the western South Urals foothills, possess relatively low relief. However, we do not see such a tendency in the Volga zircon dataset consisting of 24% Paleozoic and 76% Precambrian ages. On the other hand, the Ob' drainage area is dominated by Neoproterozoic-Phanerozoic orogenic belts of the Ural and Altai-Sayan Mountainz and, consequently, the Ob' dataset consists of 74% Phanerozoic ages. However, it also includes 26% of Proterozoic-Archean ages, but no Paleoproterozoic-Archean rocks of that age have been ever found within the Ob' catchment. Moreover, Proterozoic rocks constituting less than 2% of the drainage area are exposed within the low-relief Kazakh Uplift.

Although Cawood et al. (2003) showed that to a large extent the age spectra of river detrital zircons correspond to the basement geology, Prokopiev et al. (2008), on the example of the paleo-Lena, argued that zircons travelling thousands of kilometers from their source are not much more numerous than those from the lower reaches of the drainage system. Thus, we believe that it is not possible to conclude if main peaks on zircon age spectra depend or not on drainage basin topography, river length and flow speed.

4. Results

4.1. The Don

Sample Don-09-06 was taken at the mouth of the river, not far from a city of Rostov-na-Donu (49°12′N, 39°44′E; Fig. 1). In the concordia plot (Fig. 7a) we can recognize two tendencies: 1) a large number of zircons are plotted both on and off the curve forming two clusters of U–Pb ages at 0.9–1.2 Ga and 1.4–1.8 Ga; 2) there are also two minor clusters of points on the concordia at 300–500 Ma and 2.5–3.0 Ga. Most of the >1 Ga U–Pb ages are discordant and for the histogram they were recalculated to Pb–Pb ages (see Section 3.3). The age spectrum displays five peaks (Fig. 7b): two high Paleoproterozoic peaks at 1.9–2.0 Ga and 1.6–1.8 Ga, one Neoarchean peak at 2.6–2.8 Ga, and two smaller peaks at 0.9–1.0 Ga (Early Neoproterozoic) and 0.4–0.6 Ga (Early Paleozoic). In total, about 50% of the dataset are Paleoproterozoic ages and 20% are Mesoproterozoic (Table 2). There are also four grains older than 2800 Ma and one Mesozoic grain. Generally, the spectrum looks rather uniform implying a continuous period of granitic magmatism between 1.2 Ga and 2.3 Ga and a shorter period between 2500 Ma and 3000 Ma (Fig. 7b). The Neoarchean and Paleoproterozoic zircons were probably derived from the Ukrainian shield and Voronezh Massif, which once belonged to the Archean Sarmatia block. The Mesoproterozoic peak could be due to intracratonic rifting within the Ukrainian shield (Milanovsky et al., 1994). The Neoproterozoic peak at 0.9–1.0 Ga probably marks the Sveconorwegian orogeny related to the incorporation of EEC into Rodinia (Bogdanova et al., 2008). The Paleozoic zircons could have been derived from the Caucasus foothills, which possibly include former Late Neoproterozoic island-arc terranes at the Baltica active continental margin and collisional terranes formed during the Early Paleozoic collision of Baltica and Avalonia (Stampfli and Borel, 2002; Ruban and Yoshioka, 2005).

4.2. The Volga

Sample Vlg-1 comes from a river island located not far from the city embankment of Volgograd (48°40′N, 44°31′E; Fig. 2). We consider this sample as similar to one taken closer to the river mouth because downstream from Volgograd no notable tributaries flow into the Volga before it meets the Caspian Sea.

The Volga dataset includes only relatively concordant data (2σ uncertainty; concordance 100–98%; see Section 3). The concordia shows three main clusters of ages at 100–500 Ma, 1.0–2.0 Ga and 2.5–2.8 Ga with points plotted mainly along the curve (Fig. 7c). As was previously shown by Allen et al. (2006), who obtained 53 SHRIMP U–Pb ages for zircons from modern sand of the Volga, "given the vast area of the Volga drainage basin the age spectrum is predictably wide and diverse". Our obtained Vlg-1 histogram with PDD plot (Fig. 7d) covers a range from ca. 350 Ma to 3000 Ma and includes five main groups of ages (see also Table 2): Neoarchean (2500–2800 Ma; 10%[2]), Meso-Paleoproterozoic (1600–2000 Ma; 26%), Meso-Neoproterozoic (900–1400 Ma; 26%), Early-Middle Paleozoic (380–540 Ma; 13%) and Late Paleozoic-Mesozoic (20–310 Ma; 7%). Although it could be argued that the two Proterozoic groups represent one cluster, because the age spectrum is wide and diverse, Allen et al. (2006) also discussed similar two groups, though with caution. There are also some Mesoarchaean zircons (seven between 2800 Ma and 3000 Ma) together with occasional zircons in the period between ca. 540 Ma and 900 Ma. Only two zircons are dated as younger than 200 Ma, which is within the accuracy limit. The Volga spectrum is similar to the Don spectrum in its "Precambrian part", but different in the "Phanerozoic part", because the Don spectrum includes much fewer <500 Ma ages, which may come to the Volga basin from the Urals (Figs. 2 and 7b, d). Similarly to the Don, the Volga Archean and Proterozoic zircons were probably derived from the Voronezh and Volgo-Uralian massifs (Shchipansky et al., 2007; Bogdanova et al., 2008) as well as from the western side of the Urals comprising proto-Uralian continental blocks (Puchkov, 1997, 2003). The Early-Middle Paleozoic zircons could come from Ordovician-Devonian intermediate–acidic rocks that are widespread in the Urals, formed during subduction along the EEC margin prior to the main Baltica-Kazakhstan-Siberia collision events. The Late Paleozoic zircons—from Carboniferous-Permian granites that form the Main Granite Axis of the Urals, generated during the late stages of the Uralian orogeny (Puchkov, 1997; Bea et al., 2005).

4.3. The Ob'

We analyzed two samples OBI-SL-01 and Ob'-01-06, which were taken at the mouth of the Ob' river, not far from the city of Salekhard (66°32′N, 66°30′E; Fig. 3). The Ob' dataset is dominated by relatively concordant data (2σ uncertainty, concordance 90–100%). In the concordia plot (Fig. 8a) we can recognize three tendencies: (1) a large number of zircons are plotted along the curve and have U–Pb ages from 0.1 Ga to 1.0 Ga; (2) the zircons which have ages within two distinctive ranges of 1.0–2.0 Ga and 2.4–2.8 Ga are plotted both on and slightly off the curve; (3) there is one major (0.1–1.0 Ga) and two subordinate (1.7–2.0 Ga and 2.5–2.8 Ga) clusters of points on the concordia. The data from both samples are similar and indicate an overwhelming dominance of Neoproterozoic-Phanerozoic source rocks (68% of the whole Ob' dataset are between 100 Ma and 1000 Ma forming a huge continuous peak) with smaller older clusters at *ca.* 1.7–2.0 Ga (Late Paleoproterozoic; 13%) and 2.5–2.7 Ga (Neoarchean; 9%); there are also seven Mesoproterozoic (1.2–1.7 Ga), ten Early Paleoproterozoic (2.0–2.4 Ga) and seven Mesoarchaean (2.8–3.1 Ga) zircons (Fig. 8b). Due to the large number of analyzed zircons (N = 492) the three peaks at 100–1000 Ma, 1.7–2.0 Ga and 2.5–2.8 Ga looks very reliable suggesting three distinct periods of granitic magmatism. The huge peak at 0.3–0.9 Ga matches the crust formation of the CAOB and Uralian Orogen. The Neoproterozoic and Paleozoic zircons were probably derived from numerous granitoid terranes of the Uralian orogen (e.g., Fershtater et al., 1997), Russian Altai (e.g., Kruk et al., 1999; Vladimirov et al., 1997), Central (Heinhorst et al., 2000), Northern (Dobretsov and Buslov, 2007 and the references therein) and East Kazakhstan (Buslov et al., 2004b), Salair and West Sayan (e.g., Vladimirov et al., 1999). The Mesozoic zircons (7% of the dataset) may come from the southern Russian Altai and Chinese Altai (Vladimirov et al., 1998; Hong et al., 2004, respectively). It is still unclear where the many Archaean and Early Proterozoic ages exactly come from, because no rocks of those ages have been reliably identified within the Ob' drainage basin, except for few localities in northern Kazakhstan (Letnikov et al., 2001; Hermann et al., 2006; Kroner et al., 2007; see Section 5.5.3 for discussion).

4.4. The Yenisey

Sample Yn-01-07 was taken at the Yenisey right bank, downstream of the town of Igarka (67°26′N, 86°26′E; Fig. 1), i.e., about 300 km to the south from the river mouth, however, the Yenisey has no notable tributaries between Igarka and its mouth. The concordia shows one big cluster of points between 200 Ma and 1.0 Ga and two smaller "older" clusters at 1.7–2.0 Ga and 2.5–2.8 Ga (Fig. 8c). The most of <1 Ga data are concordant, whereas the >1 Ga data are mostly discordant. Similarly to the data from the adjacent Ob' basin (Fig. 8b), the Yenisey histogram (Fig. 8d) is dominated by Phanerozoic ages (59% of the dataset) and shows three main peaks at 0.3–0.6 Ga (Paleozoic; 54%), 0.7–0.9 Ga (Neoproterozoic; 14%) and 1.7–2.0 Ga (late Paleoproterozoic; 15%). There are also small peaks at 0.2–0.25 Ga, 2.4–2.5 Ga and 2.7–2.8 Ga. The Archean zircons were probably derived from numerous Archean terranes and blocks building the basement of the Siberian Craton, which are exposed at its southwestern frame, i.e., Sharyzhalgai and Biryusa blocks (Rosen et al., 1994). The Paleoproterozoic zircons—from a granitic belt extended along the southwestern and southern frames of the Siberian Craton including the Angara-Kan, Sharyzhalgai and Biryusa blocks of the Tunguska superterrane (Turkina et al., 2007). The Neoproterozoic zircons were probably derived from the East Angara terrane of the Circum-Siberia belt and from granitoids terranes of the Yenisey-Transbaikal belt—a part of the CAOB (Parfenov et al., 2006; Vernikovsky and Vernikovskaya, 2006; Fig. 4). The Phanerozoic zircons could come from the Middle Paleozoic Altay-Sayan and Late Paleozoic-Early Mesozoic Mongol-Okhotsk foldbelts, both branches of the CAOB. The Mesozoic zircons could have been derived from batholiths of the Hangai and Mongol-Transbaikalia continental margin units in northern Mongolia (e.g., Khentei batholith of 220–200 Ma; Yarmolyuk et al., 2001) and from the Selenga continental rift bimodal volcanic field located south and east of Lake Baikal (Kovalenko et al., 2004; Fig. 4).

4.5. The Amur

Sample Amr-01-07 was taken near the city of Komsomol'sk-na-Amure (50°31′N, 137°01′E; Figs. 1 and 5), i.e., about 350 km upstream from the Amur mouth. There is only one important tributary between the sampling site and the mouth, river Amgun, which drains the Bureya-Turana Mountains, however, big rivers Zeya and Bureya, which flow into the Amur upstream of Komsomol'sk-na-Amure, also drain the same mountain range. Therefore, we believe that the sample under study represents the whole drainage basin. The Amur concordia reveals one distinct cluster of relatively concordant ages between 50 Ma and 500 Ma and the other age points are scattered between 1.6 Ga and 2.8 Ga plotted both on and off the concordia curve (Fig. 9a). The age histogram coupled with the PDD plot shows one predominant peak at 100–200 Ma and several subordinate, though clear, peaks at 250–450 Ma, 1.8–2.0 Ga and 2.3–2.8 Ga (Fig. 9b). There are also several dates between

[2] Percentage of zircon ages of a certain time interval within a given dataset.

750 Ma and 1550 Ma and 5 results between 2.0 Ga and 2.3 Ga. The Neoarchean and Paleoproterozoic zircons were probably derived from the Bureya-Jiamusi and Argun-Indermeg basement terranes of the North China Craton (Karsakov et al., 2005). The Mesozoic and Paleozoic zircons could come from the Late Paleozoic-Mesozoic Mongolo-Okhotsk Orogen, hosting numerous granitoid complexes, e.g., Barguzin or Angara-Vitim batholith (330–290 Ma) in northern Mongolia and Transbaikalia and the Hangai (or Khangai) batholith (270–250 Ma) in west-central Mongolia and from Late Mesozoic-Cenozoic continental margin complexes of Russian Far East (Sakhno, 2001; Kovalenko et al., 2004; Fig. 5).

5. Discussion

In this section we will correlate the main peaks on detrital zircon age patterns and the major episodes of granitoid magmatism, orogeny and supercontinent assembly/breakup, addressing the question of Phanerozoic continental growth and outlining prospects for future studies.

5.1. Episodic character of continent formation

It was suggested by the episodic age distribution of juvenile continental crust, which is dominated by granitoids, that continental crust has grown during short-lived episodes in Earth history (e.g., McCulloch and Bennet, 1994; Stein and Hofmann, 1994; Condie, 1998). The global 3.3 Ga, 2.7 Ga, 1.9 Ga and 1.2 Ga peaks of continent formation were deduced from crustal zircon age distributions (Condie, 1998; Kemp et al., 2006). The episodes at 2.7–2.5 Ga and 2.0–1.9 Ga are roughly seen in all detrital zircons spectra, and those at 1.0–0.9 Ga and 0.5–0.4 Ga are present in most but not all spectra (Rino et al., 2008; Condie et al., 2009; this paper). Most igneous zircon spectra show the main peaks at 2.7–2.5 Ga, 2.0–1.9 Ga and 0.8–0.4 Ga (Condie et al., 2009).

The episodic character of continent formation possibly reflects the episodic nature of mantle dynamics as well as surface dynamics of the Earth (cf. Maruyama et al., 2007; Rino et al., 2008). During the early half of the Earth history, the felsic continental crust on the surface, which formed in an intra-oceanic environment, was mostly subducted into the deep mantle, except in the rare case of parallel arc collision of arcs (Santosh et al., 2009). At least two principal episodes of continental formation at 2.7–2.5 Ga and 2.0–1.9 Ga probably correspond to catastrophic superplume events in the mantle, which could result in crustal extraction rate exceeding crustal recycling rate (Condie, 1998, 2000; Maruyama et al., 2007). On one hand, during a superplume event the production rate of oceanic lithosphere should increase from increased ocean-floor spreading rates, and hence both sediment subduction and subduction erosion rate should also increase. On the other hand Condie (2002) argued that "...increasing rates of continental collisions may increase the rate of delamination of the lower crust. Hence, the rates of both continental crustal extraction and crustal recycling should increase during a superplume event, and if so, an increase in the net growth rate of continental crust is not necessarily expected". Condie (2002) showed that juvenile crust, at least in respect to the 1.9 Ga global event, was largely formed due to arc magmatism. Thus formed new crust was accreted to continental margins by plate collisions during the initial stages of supercontinent formation.

In any case, the recycling of continental crust has long time remained an unsolved problem. Several different models of continental growth have been proposed (Rino et al., 2004 and the references therein); however they did not take into account possible recycling of continental crust. On the basis of mass U–Pb spot dating of detrital zircons of only magmatic origin from the mouths of world largest rivers, Rino et al. (2004) estimated a new continental growth curve, which indicated major episodes of continental growth starting from the Archean. The obtained discontinuous age distribution seems to be trustworthy because the applied method minimizes the influence of recycled crustal materials and accounts for zircons almost evenly gathered from the drainage regions. A reason for the episodic character of crustal growth, which is observed in most igneous and detrital zircon spectra obtained worldwide (see a review by Condie et al., 2009), could be episodic character of arc magmatism, which is indirectly related to the episodic activity of superplumes at the core-mantle boundary (e.g., Abbott and Isley, 2002; Maruyama et al., 2007). Our new detrital zircon spectra from Russia'a major rivers confirmed the episodic character of crustal growth in global and local scales independently of the type and age of continental blocks drained by rivers.

5.2. Major peaks of granitoid magmatism and supercontinents

5.2.1. The 2.5–2.7 Ga peak: a global magmatic event

The Neoarchean peak of 2.5–2.7 Ga is seen in most so far published age histograms for detrital zircons on all the world continents (e.g., Weislogel et al., 2006; Rino et al., 2004, 2008; Allen et al., 2006; Prokopiev et al., 2008; Condie et al., 2009 and the references therein) thus marking a global event of crustal growth on the Earth (Condie, 1998, 2000; Abbott and Isley, 2002). Condie et al. (2009) wrote that the 2.7 Ga peak is the most important among the other peaks from the 2.8–2.3 Ga interval because it occurs on six or more cratons. This study showed that the 2.5–2.8 Ga peak also occurs on all the histograms (Figs. 7–9), varying within a relatively narrow interval from 4 to 12% of datasets (Table 2), thus confirming the global character of Neoarchean granitoid magmatism and crust formation. There are several hypotheses on the initiation of this event. Rey et al. (2003) proposed that that event could have been related to the crustal thickening and greenstone blanketing. The authors investigated the combined effect of greenstone cover and mantle plume, which, on their opinion, best explained the amplitude and the timing of the thermal anomaly that profoundly affected the continental crust in the Neoarchean on the basis a "mantle overturn" idea by Stein and Hofmann (1994) and the formation of plumes at the core–mantle boundary. Rino et al. (2004) discussed the mantle overturn hypothesis for the rapid growth of the continental crust based on the U–Pb ages of detrital zircons from the major rivers of North and South America. They argued that such an overturn could cause the double-layered mantle convection rather than whole mantle convection. Downwelling of subducted slabs took place into the lower mantle and induced an influx of hotter and more fertile materials from the lower into the cooled and depleted upper mantle.

The percentage of the 2.5–2.8 Ga ages in the age histograms discussed in this paper and in Rino et al. (2004, 2008) remains surprisingly stable ranging from 10 to 12 with the exception of the Yenisey histogram, which includes as little as 4% of Neoarchean zircons. Such a low percentage of Archean dates in the Yenisey dataset in spite of the oldest rocks of the Siberian Craton in the bedrock may be due to a thick Phanerozoic platform cover (Rosen et al., 1994), including flood basalts of the world famous Siberian LIP, which cover up to 25% of the catchment. We therefore believe that the presence of Archean zircons in all age spectra is almost independent of the type or age of the basement underlying a drainage basin and confirms the global character of the Neoarchean crustal growth, which probably resulted in formation of first stable continental blocks. The blocks later could become cores of large ancient continents or amalgamated into a supercontinent, e.g., the Kenorland supercontinent of Williams et al. (1991) or the Arctica supercontinent of Rogers and Santosh (2003).

5.2.2. The 1.7–2.0 Ga peak: Columbia supercontinent

The Paleoproterozoic peak is also present in all the zircon age histograms (Figs. 7–9). Condie et al. (2009) recognized three major episodes of granitoid production within the 2.3–1.5 Ga interval: 2.15–2.0 (Africa, South America, Siberia, Australia, East Asia and Antarctica), 1.85–1.95 Ga (East Asia, South America, Laurentia, Australia and Africa), and 1.8–1.55 Ga (Laurentia, Australia and Africa). Our detrital data (Don and Volga–Europe/Baltica/EEC, Ob' and Yenisey–Siberia and CAOB, Amur–Siberia and East Asia) show no data matching the first episode. The second episode is present in all the histograms and the third episode is seen in the Don and Volga (EEC) histograms only (Figs. 7 and 9), implying a different history of terrane/block collisions within the EEC compared to the Siberian Craton and Gondwana-derived microcontinents incorporated in the CAOB. Therefore, we conclude about a global episode of granitoid magmatism at 1.8–2.0 Ga and believe that this peak is consistent with the hypothesis of the global assembly of Paleoproterozoic continents into the Columbia supercontinent as was proposed by Rogers and Santosh (2002) and Santosh et al. (2009). This hypothesis stands on the worldwide distribution of 1.8 Ga orogenic belts (Condie, 2002) and on the synthesis of recent petrologic and geochronological data suggesting the amalgamation of Columbia between 1.85 Ga and 1.9 Ga (Rogers and Santosh, 2009). This peak probably marks a coherent event of orogeny and voluminous granite-granodiorite magmatism (Santosh et al., 2009), which affected the entire Earth. We suggest the breakup of Columbia at 1.3–1.2 Ga according to the small amount or absence of those age data in most age spectra (Figs. 7–9). Thus, our data may contribute to the Columbia supercontinent model.

5.2.3. The 0.9–1.1 Ga peak: Rodinia supercontinent and Grenvillian orogeny

The Rodinia supercontinent is thought to be assembled during a time interval from 1.3 Ga to 0.9 Ga and to include almost all the continents of the world (e.g., McMenamin and McMenamin, 1990; Condie, 2001; Maruyama et al., 2007; Li et al., 2008). The Grenvillian orogeny (ca. 1.0 Ga) is also thought to be worldwide and closely related to the reconstruction of Rodinia. The events of Rodinia assembly and its related Grenvillian orogeny are seen in many, but not all, detrital zircon spectra obtained worldwide. Most of the zircon populations obtained from 13 world largest rivers (Rino et al., 2008) show the presence of Grenvillian zircons (1.0–1.1 Ga). However, the PDD plots and histograms obtained from Asia (Ob', Yenisey and Amur) do not record Grenvillian age granitoid/orogeny events (Figs. 7–9). Amongst the published data no notable peaks from the 1.3–0.9 Ga interval are observed in the histograms for East Asia (Condie et al., 2009) and Siberia (paleo-Lena river in Prokopiev et al., 2008; river Ob' in Rino et al., 2008). Our data show clustered data in the 0.9–1.0 Ga and 0.9–1.2 Ga intervals in the Don and Volga histograms, respectively (Figs. 6 and 8), but a clear "Rodinia-Grenvillian" peak in the Volga histogram only (25% of the dataset). This peak probably reflects the Baltica-Laurentia collision at 1.0 Ga according to Li et al. (2008), who argued that at 1.1 Ga Laurentia, Siberia, North China, and South China were already together. This idea explains the absence of Grenvillian ages in the Ob' (partly), Yenisei, and Amur histograms in this study and in the paleo-Lena histogram from Prokopiev et al. (2008). This is because the evolution of these drainage basins is related to the reconstructions between Siberia and North China, whereas the evolution of East Asia is closely tied with the collision between North and South China. Therefore, the absence of Grenvillian peaks in the Yenisei and Amur age histograms (Figs. 8 and 9) and in the East Asia PDD plots (Condie et al., 2009) supports the idea of early amalgamation of those continental blocks, which did not resulted in worldwide orogeny however. Thus, our new data together with those reported by Gladkochub et al. (2006), do not confirm the global character of Grenvillian orogeny, at least in respect to Siberia/Asia.

5.2.4. The 0.8–0.5 Ga peaks: Gondwana supercontinent and Pan-African orogeny

If the Grenvillian orogeny records the reconstruction of Rodinia, the Pan-African orogeny, which was also an important period in the Earth's history at the Precambrian-Phanerozoic boundary, marks the assembly of Gondwana. Hoffman (1991) first suggested that the breakup of Rodinia involved fragmentation of Laurentia into continental blocks, which later were amalgamated on the other side of the Earth to form the Gondwana supercontinent by ca. 540–530 Ma (e.g., Collins and Pisarevsky, 2005; Meert and Lieberman, 2008; Stern, 2008). Gondwana presumably formed during a period from 600 Ga to 540 Ma and involved collision of East and West Gondwana and formation of Pan-African orogenic belts worldwide (Rino et al., 2008).

After the final assembly numerous small blocks or microcontinents were rifted off East Gondwana and drifted away to collide together or large continents. For example, the Kokchetav (Ob' basin), Altai-Mongolian (Ob' and Yenisey basins) and Tuva-Mongolia (Yenisey and Amur basins) microcontinents separated from East Gondwana during the Late Neoproterozoic and collided with the Siberian Craton during the Early Paleozoic; later, in the Late Paleozoic, Siberia collided with the Kazakhstan block (e.g., Buslov et al., 2001, 2004a; Dobretsov and Buslov, 2007).

The Pan-African orogeny is seen in most PDD plots and histograms of detrital zircons worldwide (Rino et al., 2008; Condie et al., 2009). Condie et al. (2009) discussed two episodes of supercontinent assembly in the 0.8–0.5 Ga interval: 750 Ma (Laurentia: Africa and Siberia) and 540 Ma (Gondwana: Europe, East Asia, South America and Africa). Our data show no peaks at 750 Ma in the Don–Volga (Europe) and Amur (East Asia) histograms, but do in the Ob' and Yenisey histograms (Figs. 7–10). However, the 540 Ma peak, Gondwana assembly, is present in the Ob' histogram only. Thus, our new data do not confirm the global character of the Pan-African orogeny in connection with the assembly of Gondwana in Eurasia.

5.2.5. Middle-Late Paleozoic peaks: Pangea supercontinent?

If we accept the idea that formation of supercontinents is recorded in peaks of detrital zircons samples worldwide, like those at 2.5–2.8 Ga (Kenorland), 1.7–2.0 Ga (Columbia), 1.0–0.8 Ga (Rodinia), 0.6–0.55 Ga (Gondwana), which are seen in most, but not all, detrital zircon age spectra, we should expect a "Pangea" peak at around 0.4–0.3 Ga (Cock and Torsvik, 2007) or 0.25–0.2 (Santosh et al., 2009). Generally, the Paleozoic-Mesozoic ages are present in all "Asian" histograms, however their percentage is greatly variable and the clear peaks are rare (Table 2; Figs. 8–10b–d). The Late Paleozoic "bins" are usually parts of big Late Neoproterozoic-Paleozoic peaks (Early Paleozoic peaks are discussed in Section 5.3) suggesting continuous granitoid magmatism. Three supercontinents, Rodinia, Gondwana and Pangea, assembled and broke during the last 1 Ga. We cannot recognize clear "Rodinina", "Gondwana" or "Pangea" peaks in the "Asian" histograms. If this is because the events of continental assembly and breakup are closely accompanied by multiple episodes of oceanic accretion, collision and intraplate magmatism?

The Late Paleozoic ages are found in the Volga histogram only, obviously due to the events of active margin magmatism and later collision between the EEC and Kazakstan block. Later the composite EEC and the Siberian Craton were amalgamated to form Pangea. In the Ob', Yenisey and Amur catchments the Late Paleozoic zircons can be attributed to the evolution of the CAOB, which will be discussed in Section 5.3.

In most models the formation of Pangea is reconstructed for the period between 400 Ma and 300 Ma. Pangea's status as a supercontinent has long been debated based on whether or not all the continents were amalgamated together during this time (Murphy et al., 2009; Santosh et al., 2009 and the references therein) or whether Pangea had a 'close packing' of all the continental fragments on the globe as proposed for large supercontinents like Columbia (cf. Rogers and Santosh, 2002). It was suggested that the southern part of this landmass has a dispersion history, and the northern part has an amalgamation history. The northern part of Pangea, Laurasia, was rather rapidly assembled by a series of collision events including Baltica, Siberia, North China, Kazakhstan, and some Gondwana-derived blocks (450–250 Ma) followed by Pacific subduction. Our data suggest a continuous amalgamation of Asia, which probably ceased in the Early Mesozoic, approximately after 200 Ma, after which the Pacific-type orogeny dominated in East Asia.

5.3. Phanerozoic granitoid magmatism events and crustal growth in the CAOB

The Phanerozoic period of granitoid magmatism in Central Asia is seen in all "Asian" spectra and is largely related to the formation of the CAOB, which started in the Late Neoproterozoic-Early Paleozoic due to oceanic closure, accretion and collision accompanied by suprasubduction and collision-related felsic magmatism. The 450 Ma peak reflecting accretion processes in the Paleo-Asian ocean realm (Safonova et al., 2009b) is seen in all the spectra except for the Amur's. The western part of the CAOB, which is present within the Ob' drainage basin, formed during the Early Paleozoic collision of the Gondwana-derived Kokchetav and Altay-Mongolian microcontinents with the Siberian Craton (Buslov et al., 2001; Dobretsov and Buslov, 2007). The eastern part of the CAOB was formed during the Middle Paleozoic collision of the Gondwana-derived Tuva-Mongolian microcontinent and Siberian Craton (Didenko et al., 1994). Paleozoic granitic intrusions of orogenic, syn- and post-collisional and intraplate origin (Kovalenko et al., 2004; Yarmolyuk et al., 2001; Yarmolyuk and Kovalenko, 2003) are distributed mainly in the northern part of the CAOB (Transbaikalia). They include (1) numerous granodiorite–granite plutons of the calc-alkaline series intruded at 500–440 Ma, i.e., during and after collision of Precambrian microcontinental blocks and island arcs of the Paleo-Asian ocean; (2) Late Ordovician–Devonian (440–360 Ma) granodiorite-granite and andesite-dacite-rhyolite units of the Altai-adjacent active continental margin of the Siberian Craton; (3) Carboniferous and Permian calc-alkaline granitoid magmatism in northern Mongolia and Transbaikalia (e.g., the 330–290 Ma Barguzin batholith; Kovalenko et al., 2004).

The huge Early-Middle Palaeozoic peak in the Ob' and Yenisey spectra (22 and 43% of the two datasets, respectively) matches the Altaid/CAOB crustal growth event very well. However, it is not seen in several published models for crustal evolution based on zircon age peaks (Condie, 1998; Kemp et al., 2006). Moreover, the most age spectra presented in Condie et al. (2009) lack the Phanerozoic part. We pose the question: have some researchers underestimated the amount of Phanerozoic crustal growth/orogenesis because they did not work in Central Asia or the CAOB? Central Asia is a complex mosaic of dominantly accretionary, island-arc and continental margin complexes, interspersed with older continental blocks and fragments of oceanic crust. In contrast with the Caledonian, Hercynian and Himalayan orogenic belts that resulted from frontal collision of Precambrian cratonic blocks, which have been studied in details, the CAOB grew at the expense of subduction–accretionary complexes and their splitting along strike-slip faults (Jahn, 2004). The isotopic dating of granitoids of the CAOB performed during the last 10 years allowed researchers to develop a general scenario of massive juvenile crust production in the CAOB with limited influence of old microcontinents in the genesis of Phanerozoic granitoids and to show that the CAOB was the world's largest site of juvenile crustal formation in the Phanerozoic eon (e.g., Sengör et al., 1993; Kovalenko et al., 2004; Jahn et al., 2004 and the references therein). We believe that the presented data are indicative of an important period of continental growth during the Phanerozoic and must be included into available/popular models of global continental growth. However, to confirm the juvenile crustal growth in Central Asia Lu-Hf isotope analysis of the same zircons may be necessary.

5.4. Mesozoic and Cenozoic zircon ages

The amount of Mesozoic ages in the Don and Volga datasets is below the analytical accuracy (see Sections 4.2 and 4.3; Table 2).

Mesozoic magmatic activity in the CAOB resulted from processes of accretion and collision of the Siberian Craton, Precambrian possibly Gondwana-derived microcontinents, Early and Late Paleozoic foldbelts of the CAOB and the North China Craton accompanied by intensive intraplate activity. The Ob' and Yenisey age histograms show no clear Mesozoic peaks, although the datasets include 7 and 5% of Mesozoic ages, respectively (Table 2, Fig. 10b). Within the Ob' catchment the Permian-Triassic and Triassic-Jurassic rifting-related granitoid magmatism was reported for the Russian Altai (Vladimirov et al., 1997). Some authors believe that the rifting was related to mantle plumes (Buslov et al., 2007).

In the Yenisey basin the Mesozoic granitoides occur in Northern Mongolia and Eastern Transbaikalia (Badarch et al., 2002; Yarmolyuk and Kovalenko, 2003). During this period, within the Amur catchment, the Late Paleozoic Hangai batholith (270–250 Ma), the Early Mesozoic Khentei (220–200 Ma) and Late Mesozoic Uda-Stanovoy (150–120 Ma) batholiths of Transbaikalia and northwestern Mongolia (Figs. 4 and 5) were emplaced (Kovalenko et al., 2004). The clear peak at 100–200 Ma in the Amur histogram (Figs. 9b and 10c) obviously marks the intracontinental rift/plume related magmatism (Mongolia) and continental margin magmatism (Russian Far East) as a result of subduction of the Pacific oceanic plate beneath the East Asia continental margin (Fig. 5; Maruyama et al., 1997), because in the last 200, no continent has collided and amalgamated to become part of East Asia, except for the accretion of oceanic materials (Santosh et al., 2009). Single dates younger 100 Ma (two grains in both the Ob' and Amur histograms) are within the accuracy of the method and are out of consideration.

5.5. Cumulative histograms, groups of continents and history of continent collisions

In this section we will discuss statistical results of comparison of all age datasets and consider three groups of age data. The comparison will be based on cumulative histograms compiled using the age data from five rivers normalized to 100% within each bin. The statistical comparison of U–Pb detrital zircon age distributions is needed because visual comparison of two and more distributions by looking at histograms or probability density functions, can be quite subjective.

5.5.1. Comparison of detrital zircon age distributions using the K–S test

We used the Kolmogorov–Smirnov (K–S) test to assess the similarity of the distributions of single grain ages. The K–S test is a means to mathematically compare two distributions and determine if there is a statistically significant difference between the two distributions. In our case it was used as a non-parametric method for comparing cumulative probability distributions – CPD (Press et al., 1986). The K–S test tests the null hypothesis that

Table 3
P- and *D*-values with error in the CDF calculated using the Kolmogorov–Smirnov test as an Excel macro (Press et al., 1986).

	P-values using error in the CDF				Volga
	Don	Amur	Yenisey	Ob'	
Don		0.000	0.000	0.000	0.000
Amur	0.000		0.000	0.000	0.000
Yenisey	0.000	0.000		0.002	0.000
Ob'	0.000	0.000	0.002		0.000
Volga	0.000	0.000	0.000	0.000	
	D-values using error in the CDF				Volga
	Don	Amur	Yenisey	Ob'	
Don		0.611	0.607	0.568	0.362
Amur	0.611		0.436	0.436	0.495
Yenisey	0.607	0.436		0.169	0.420
Ob'	0.568	0.436	0.169		0.375
Volga	0.362	0.495	0.420	0.375	

Zero *P*-values mean that a sample is rejected as being too different from every other sample. The higher is *D*-value, the greater is difference between samples. According to these criteria we can statistically join Ob' and Yenisey samples only ($P = 0.002$, $D = 0.169$). However, we also join Don and Volga samples because they drain the same craton (EEC) and have not very high *D*-value (0.362).

the two distributions are the same. Specifically, the K–S test compares the maximum probability difference between two CPDs. If this observed difference, D_{obs}, is greater than some critical value, D_{crit}, the null hypothesis is rejected and the two samples most likely did *not* come from the same population (e.g., detrital zircons in two samples were not shed from the same source region). Table 3 presents *P*- and *D*-values (*D* is, simply speaking, $D_{obs} - D_{crit}$) for all possible pairs of datasets. The *P*-value is the probability that the observed D_{obs} could be due to random error.[3] Zero *P*-values mean that a sample is rejected as being too different from every other sample. The higher is *D*-value, the greater is difference between samples. According to these criteria we can statistically join Ob' and Yenisey samples only ($P = 0.002$, $D = 0.169$). However, we also resolved to join Don and Volga samples because they drain the same craton (Baltica or EEC) and have not very high *D*-value (0.362). So, we joined the Don and Volga results into Group 1, the Ob' and Yenisey results into Groups 2 and 3 is the Amur zircon population (Table 3). Thus, we will consider three groups of zircon ages (Fig. 10): Don–Volga or Baltica Group (Sarmatia and Volgo-Uralia continental blocks, Scythian platform, Uralian and Caucasian orogens), Ob'-Yenisey or Siberia Group (Siberian Craton, CAOB, Kokchetav, Altay-Mongolian and Tuva-Mongolian microcontinents), and Amur or East Asia Group (Siberian and Sino-Korean Cratons, Mongol-Okhotsk and Sikhote-Alin orogenic belts).

5.5.2. Don–Volga cumulative histogram: East European Craton and Uralian orogen

The Don and Volga spectra look similar and have common peaks at 2.6–2.8 Ga, 1.9–2.0 Ga and 1.6–1.8 Ga, but different younger parts of the spectra (Fig. 10a). The wide range of Precambrian ages in the Don and Volga river samples is consistent with the polyphase evolution of the EEC. The absence of zircons older than ca. 2900 Ma in the Volga samples but their presence in the Don sample matches the scarcity of Archaean crust of 3 Ga age in the Volgo-Uralia Block (Bogdanova, 1986) but its presence in the Sarmatia Block (e.g., Bibikova and Williams, 1990; Samsonov et al., 1996). Our data confirmed the previously proposed idea that Archean crust does not appear to have contributed significantly to the Phanerozoic deposits of the EEC (Allen et al., 2006). The Don histogram includes more Paleoproterozoic and fewer Paleozoic ages (Table 2; Figs. 7b and 10a), because its bedrock is dominated by Sarmatia units compared to the Volga which catchment includes Volgo-Uralia units (see Section 2; Table 1).

The cluster of ages between ca. 2.0 Ga and 1.9 Ga marks the collision of Sarmatia and Volgo-Uralia (Bogdanova et al., 2008 and the references cited therein), which is a manifestation of a global orogenic/granite-granodiorite event related to Columbia amalgamation (Rogers and Santosh, 2002; Santosh et al., 2009; see Section 5.2). Bogdanova et al. (2008) believe that the assembly of the EEC began at 2.0 Ga when Sarmatia and Volgo-Uralia joined each other to form the Volgo-Sarmatian protocraton, which existed as a separate unit until ca. 1.8–1.7 Ga when it docked with Fennoscandia and a unified craton was created. The 1.8–1.6 Ga peak seen in both histograms suggests that Volgo-Sarmatia existed as a separate craton until maximum 1.8 Ga and obviously marks the final amalgamation of the EEC (Fig. 10a).

The cluster of Mesoproterozoic ages between 1400 Ma and 1600 Ma (Fig. 10a), when the EEC appears to have been part of the Columbia supercontinent, probably mark several important events of orogeny and its related intracratonic magmatism (Bogdanova et al., 2008). Milanovsky et al. (1994) believe that those events were probably related to the Riphean multi-stage intracontinental compression of the EEC. The important period between 1.5 Ga and 1.4 Ga, when substantial regions in the western part of the EEC were affected by igneous activity, metamorphism and deformation, is the "Danopolonian Orogeny" after (Bogdanova et al., 2008).

The 1.4–1.2 Ga interval defines the rifting of the EEC crust, which resulted in sill intrusions of both mafic and felsic compositions in the South Urals (Alekseev, 1984). The 1.3–1.4 peak in the Volga histogram coincides with the 1.39–1.38 Ga Sm–Nd ages of South Uralian volcanics, subvolcanics and intrusions (Bogdanova et al., 2008). It is less evident in the Don histogram, but possibly marks later intracontinental compression (Milanovsky et al., 1994).

The 0.9–1.0 Ga and 0.9–1.1 Ga peaks in the Don and Volga histograms, respectively (Fig. 10a), correlate reasonably well with the Grenvillian orogeny, however, exposed basement with such characteristics lies far from the modern drainage basins. Milanovsky et al. (1994) believe that the EEC experienced the third stage of Riphean compression at that time. On the other hand, these peaks probably mark the collision of the EEC and Amazonia (Nikishin et al., 1996; Bogdanova et al., 2008) to become parts of Rodinia (Li et al., 2008).

Paleozoic ages are typical of the Volga histogram (Fig. 10a). The 0.5–0.25 Ga peak (20% of the dataset) obviously marks the magmatism in the southern Urals developed in relation to the probable Early Carboniferous collision of the Kazakhstan block with the Uralian arc-trench system (Nikishin et al., 1996) and Late Carboniferous collision of the evolving Uralian orogen with the southeastern part of the EEC passive margin (Puchkov, 1997). The Volga histogram includes mid-Carboniferous to Late Permian zircons (6% of the dataset; Table 2; Figs. 7d and 10a), although Allen et al. (2006) mentioned their absence. This is the age range of the granites that form the Main Granite Axis of the Urals, generated during the late stages of the Uralian orogeny (Fershtater et al., 1997; Puchkov, 1997). Therefore we believe that there really has been late Palaeozoic and post-Palaeozoic contribution from these granites to the cover of the EEC. There are few Mesozoic grains in the Don and Volga datasets (Figs. 7b, d and 10a), which is less than 2% of the datasets, i.e., below the analytical accuracy.

5.5.3. Ob'–Yenisey cumulative histogram: Siberian Craton, CAOB and Uralian Orogen

The cumulative Ob' and Yenisey histogram has peaks at 2.5–2.8 Ga, 1.7–2.0 Ga and 0.2–0.7 Ga (Fig. 10b). The Neoarchean

[3] The smaller the *P*-value, the less likely that the observed D_{obs} is due to random error and the more likely that the difference is because the distributions are not the same (Guinn, 2006).

ages (2.5–2.8 Ga) are typical of both basins and constitute 9 and 4% of Ob' and Yenisey datasets, respectively (Table 2). However, the area of exposed Neoarchean rocks differs from 0% for the Ob' basin to 4–10% according to different evaluations (Nalivkin, 1983; Rosen et al., 1994), for the Yenisey. The Paleoproterozoic peak at 1.7–2.0 Ga constitutes 13 and 15% of the Ob' and Yenisey datasets, respectively. The area of the exposed rocks of that age is also 0% for the Ob' basin and ca. 7% for the Yenisey. The Neoarchean and Paleoproterozoic zircons in the Yenisey basin, 20% of the dataset (Table 2), were probably derived from Early Precambrian basement blocks, e.g., Angara-Kan, Birusa and Sharyzhalgai (see Section 2.3; Figs. 3 and 4).

However, it is still unclear where the many Archean and Paleoproterozoic ages in the Ob' dataset come from exactly, because no rocks of those ages have been reliably identified within the drainage basin. Shatsky et al. (1995) reported about Archean Sm-Nd models ages for the Kumdy-Kol diamondiferous gneisses in northern Kazakhstan, Kokchetav Massif. Proterozoic U–Pb ages have been recorded in the cores of metamorphic zircons of the Kokchetav Massif (Claoue-Long et al., 1991; Letnikov et al., 2001; Hermann et al., 2006; Kroner et al., 2007). Besides Necheukhin et al. (2000) and Fershtater et al. (2009) reported about Paleo- and Mesoproterozoic ages of zircons from small continental blocks or terranes in the southeastern Urals. As far as the Ob' spectrum contains many Archean ages, 10% of the dataset, we suggest that the primary oldest rocks in the Ob' basin can be found either in the southeastern Urals and/or in North Kazakhstan; the latter region hosts the oldest cratonal block, Kazakhstan, in the region exposed. Anyway those basement blocks may be source of recycled or so far unidentified Archean and Paleoproterozoic terranes.

Both the Ob' and Yenisey histograms have big Neoproterozoic-Paleozoic peaks, 61 and 68% of the two datasets, respectively (Table 2). These peaks match the subsequent assembly of Rodinia (1.0–0.9 Ga) and Gondwana (550–530 Ma) and crustal growth of the CAOB (see Sections 5.2 and 5.3). In the Ob' basin (Fig. 3) the Neoproterozoic terranes occur in the East Uralian block/microcontinent (Necheukhin et al., 2000), Gornaya Shoriya (Vladimirov et al., 1999), and Chinese Altai (Windley et al., 2002).

The Paleozoic zircons were probably derived from Altay-Sayan orogenic belts formed during the main stage of the formation of the Central Asian Orogenic Belt (Jahn et al., 2000; Yarmolyuk and Kovalenko, 2003; Kovalenko et al., 2004; Kroner et al., 2007). The CAOB was formed during the amalgamation of Gondwana-derived continental blocks, e.g., Kokchetav, Altay-Mongolian, Tuva-Mongolian (Buslov et al., 2001), etc., and terrains of different geodynamic origin, such as ophiolites, island arcs, and active margin units and overlapped Transbaikalian magmatic arcs (Figs. 3 and 4). Some of those terranes developed in response to subduction of the oceanic crust of the Paleo-Asian Ocean, which started in the Late Neoproterozoic in its western branch and finished in Late Carboniferous-Permian in its eastern branch (Dobretsov et al., 1995; Buslov et al., 2004a; Safonova et al., 2009b).

5.5.4. *Amur normalized histogram: Siberian and Sino-Korean Cratons, Mongol-Okhotsk and Sikhote-Alin Orogens*

The Amur age histogram displays three major peaks: at 2.3–2.6 Ga, 1.8–2.0 Ga and 0.1–0.4 Ga (Table 2, Figs. 9 and 10c). The global Neoarchean and Paleoproterozoic peaks are typical of the Amur basin, likewise of the other basins, and constitute 10 and 8% of the dataset, respectively. These values roughly match the areas of exposed rocks of those age intervals. The Neoarchean-Paleoproterozoic zircons could have been derived from the Argun-Indermeg and Bureya-Jiamusi continental blocks and Circum-Siberian belts (Fig. 5). The peak at 0.2–0.4 Ga corresponds to the Late Paleozoic-Mesozoic granitoid magmatism and felsic volcanism of the Hangai and Selenga overlap continental margin arcs and Mongol-Okhotsk orogen, the youngest orogenic belt in the region, which formed due to the collision of the Siberian Craton with the Sino-Korean craton and Gondwana-derived Argun-Idermeg continental block. The largest peak between 100 Ma and 200 Ma (40% of the dataset; Fig. 10c) marks the Late Mesozoic-Cenozoic granitoid magmatism of the Badzhal, Sikhote-Alin and Uda-Stanovoy island-arc and continental margin units (Fig. 5). Formation of continental margins volcano-plutonic belts and arcs over ancient basement is related to the subduction of the Pacific plate beneath the East Asia continental margin (Sakhno, 2001; Jahn et al., 2004; Karsakov et al., 2005).

Of special interest is few, if any, zircons in the age interval between 0.5 Ga and 1.8 Ga. This confirms the youngest age of North-East Asian granitoid/orogenic belts compared to the rest of Eurasia. Based on this gap we suggests that the old continental blocks present in this area, the Argun-Indermeg and Bureya-Jiamusi superterranes and the northern margin of the Sino-Korean craton, did not experience of Grenvillian and Pan-African orogenies, which were previously regarded as global.

The age histogram of the Yellow river (Rino et al., 2008), which basin is adjacent to the Amur's in the north, is characterized by a different "peak pattern": there are two wide peaks at 0.1–1.0 Ga and 1.5–2.0 Ga and a high peak at 2.3–2.5 Ga. The age spectrum of the paleo-Lena (Middle Jurassic), which neighbours the Amur basin in the southeast, is characterized by three main peaks at 0.2–0.3 Ga, 0.4–0.5 Ga and 1.8–2.0 Ga and a small peak at 2.5–2.6 Ga (Prokopiev et al., 2008), i.e., generally similar to that of the modern Amur. Moreover, the Mesoproterozoic "pause" of granitoid magmatism within and around the Siberian Craton (Figs. 8d, 9b, and 10b, c; Prokopiev et al., 2008) is confirmed by the pause in mafic magmatic in the same area. Evidenced for this comes from the isotope dating of mafic rocks (Gladkochub et al., 2010). This indirectly confirms the "independent behaviour" or an isolated position of the Siberian Craton compared to the other Rodinia derived continental blocks (e.g., Zonenshain et al., 1990; Scotese, 2004; Cocks and Torsvik, 2007).

5.6. *Formation of supercontinents and tectonics: prospects for future studies of detrital zircon ages*

The detrital zircon age spectra/histograms represent a powerful instrument for studying the episodic character of continental growth, its rate, and global and local episodes of orogeny in paleo- and modern drainage basins, which bedrocks consist of cratonic blocks and their separating orogenic belts. The previous studies (e.g., Rino et al., 2004, 2008; Condie et al., 2009 and references therein) showed that most age spectra obtained worldwide have both common and different features. The common features may be due to the global processes of continent growth which occurred on almost all earth continents. The differences may come from different parental supercontinents, from which the blocks composing the relevant drainage areas were split off. For example, the Baltica (Don and Volga) and Siberia (Ob' and Yenisey) and Sino-Korea (Amur) cratons had different histories before they amalgamated with different continents at different times to form the Rodinia supercontinent (Bogdanova et al., 2008; Li et al., 2008; Santosh et al., 2009). The Ob' and Yenisey zircon age populations carry not only Rodinia and Gondwana signatures but reflect granitoid magmatism related to oceanic subduction and accretion, continental collision and post-collisional orogeny (Buslov et al., 2001, 2004a; Dobretsov and Buslov, 2007; Safonova et al., 2009b). Accepting that the major events of crustal growth happened before the Mesoproterozoic (Condie, 2002; Condie et al., 2009; Rogers and Santosh, 2002, 2009; Rino et al., 2004, 2008), we believe that the "Archean parts" of age spectra reflect the history of protocontinents which gave birth to the continents later amalgamated to form the Columbia, Rodinia

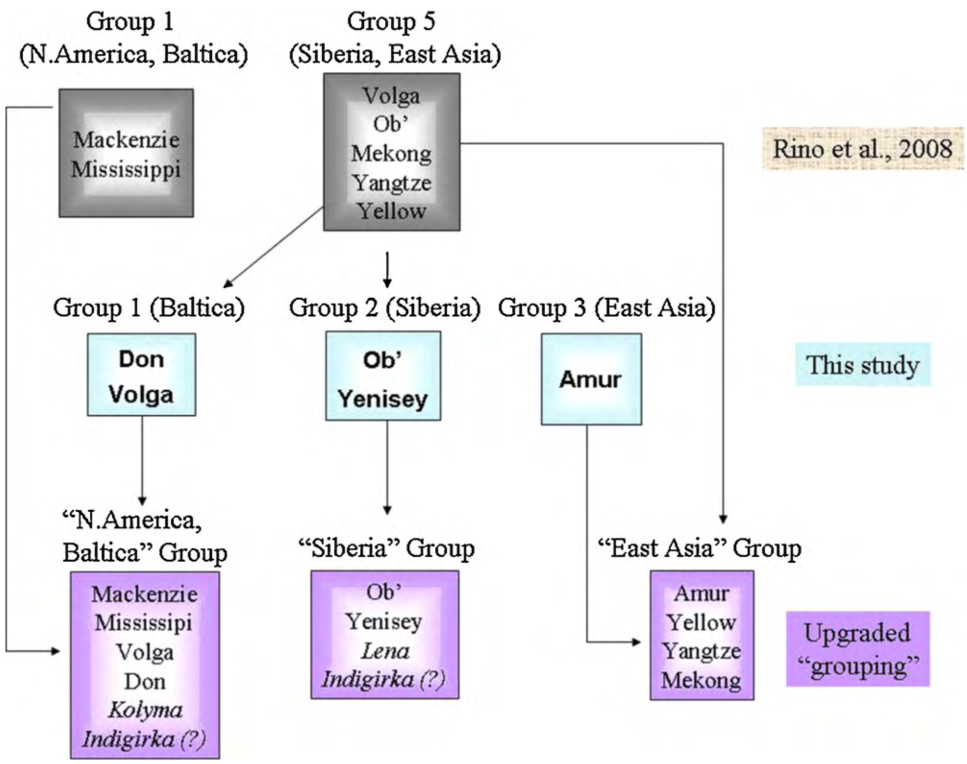

Fig. 11. Block diagram showing the former and upgraded grouping of continents and relevant detrital zircon data from world major rivers (the names of rivers for future studies are given in italic).

and Gondwana supercontinents. The "younger parts" of the spectra reflect periods of oceanic subduction/closure, accretion and continental collision accompanied by active continental margin and collisional magmatism rather than the main episodes of supercontinent assembly and breakup.

We compared the three groups of data, Baltica, Siberia and East Asia, with the groups regarded in Rino et al. (2008): North America-Baltica (Group 1), West Africa-South America (Group 2), Antarctica-Africa (Group 3), Australia (Group 4) and Asia (Group 5). In this paper we join our Baltica Group (Don and Volga) with Group 1 (North America-Baltica) from Rino et al. (2008) and distinguish a separate Siberia Group, which will include the data on the Ob' and Yenisey basins. Thus, we propose to "upgrade" Group 5 from Rino et al. (2008) to exclude the Volga and Don results and to split it into two groups: Siberia (Ob', Yenisey, Lena) and East Asia (Amur, Yellow, Yangtze, Mekong). A reason for such a subdivision is that the Siberian group histograms (Fig. 10b) are characterized by the dominating Neoproterozoic-Paleozoic peak, whereas the East Asia Group (Fig. 10c) is special for a high portion of Mesozoic ages, which is supported by statistical processing of the results (Section 5.5.1; Fig. 11). Moreover, we mentioned above that some researchers believe that the Siberian Craton obviously had a history different from that of East Asia cratons, i.e., North and South China (see also Section 5.5.4; Scotese, 2004; Cocks and Torsvik, 2007).

Thus, the results presented in this paper cannot unambiguously resolve two main questions: (1) Did the Grenvillian and Pan-African orogenies have really global characters? and (2) Was Pangea a "true" supercontinent? Obtaining results from the Lena, Indigirka and Kolyma rivers in North-East Siberia would be an important contribution to this. If/when we obtain results on the Lena, a great river in Siberia draining the Siberian Craton (4400 km long and about 2.5 million km^2 in catchment area), we will join them with the Siberia Group results. The Kolyma and Indigirka rivers drain the Kolyma-Omolon terrane, which origin has long time remained a subject of debate in respect its relation to the Siberian and North American Cratons. The detrital zircon age data on these river basins would help us to shed light on the origin of North-East Siberia—one of the most mysterious and hardly accessible regions of the world. We believe that study of these river basins could shed light on relationships between continental blocks composing North-East Asia and North America. In future those data could be included in Group 1 from Rino et al. (2008), i.e., North America plus Baltica, or in Group 2, i.e., Siberia (Fig. 11). Another perspective of research is analysis of Hf isotopes in the same zircon grains, which have been analyzed for their U–Pb age in order to confirm or decline the juvenile character of the crustal growth in Central Asia and other regions.

More prospects for future studies lie in the comparison of detrital zircon age data from modern and older sand/sandstone units in order to find out main stages of tectonic reorganization and terrane exposure. Our first results of that kind on the Ob' basin showed that the age spectrum of a Paleogene sand contain few, if any, Phanerozoic zircons. We tentatively suggested either an ancient continental block, which, before ca. 30 Ma, was uplifted to isolate the provenance from Phanerozoic orogens, or the uplifting of Phanerozoic granitoids in Central Asia after 30–35 Ma, possibly as a result of the India-Eurasia collision, which reactivated orogeny in Altay-Sayan and Kazakhstan (Safonova et al., 2009a).

6. Conclusions

LA ICP MS U–Pb isotope dating of detrital zircons from modern sand of world major rivers was proved to be a powerful method for reconstructing global events of continental crust formation and growth, amalgamation and breakup of supercontinents and recognizing major peaks of orogeny.

Our data allowed us to re-confirm (1) the cyclic character of continental growth; (2) the global character of the Neoarchean event of magmatism related to a global event in the mantle and, possibly, formation of the Kenorland supercontinent; (3) the global character of the crust formation at 2.0–1.7 Ga, which resulted in the assembly of the Columbia supercontinent; (4) the breakup of Columbia at 1.3–1.2 Ga according to the small amount of those ages in most histograms.

On the other hand, we could not confirm the global character of the Grenvillian and Pan-African orogenies related to the formation of the Rodinia and Gondwana supercontinents. The “Rodinia” peaks are not observed in the Ob’, Yenisey and Amur, i.e., in “Asian”, histograms (Groups 2 and 3), whereas the “Gondwana” signature in not obvious in the Don, Volga and Amur histograms (Groups 1 and 3; Fig. 11).

Of special interest are the 2.7–2.5 Ga and 2.0–1.7 Ga peaks in the Ob’ age histogram/spectrum in spite of the absence of reliably identified rocks of those ages within the Ob’ drainage basin. This suggests that Neoarchean-Paleoproterozoic rocks can be found by more comprehensive geochronological study of granitoids exposed in this region.

The obtained age results contribute to the idea about the Phanerozoic juvenile crustal growth in Central Asia (e.g., Sengör et al., 1993; Jahn, 2004), which resulted from oceanic subduction, accretion, syn- and post-collisional and intraplate magmatism.

For further reconstructions we propose to join the U–Pb detrital zircon data from Russia to the following detrital zircon age groups from other world regions: (1) North America and Baltica, to include the Mississippi, Mackenzie, Don, Volga, Kolyma and possibly Indigirka; (2) Siberia, to include the Ob’, Yenisey and Lena and possibly Indigirka; (3) East Asia, to include the Amur, Yellow, Yangtze and Mekong.

The prospects for future studies lie in the dating of detrital zircons from the Lena, Kolyma and Indigirka rivers in Russia for more continental growth implications, comparing detrital zircon ages from modern river sand and paleo-sandstones within a given drainage basin for tectonic reconstructions, and analyzing Lu-Hf isotopes in the dated zircons for confirming/declining the juvenile character of crustal growth in Central Asia.

Acknowledgments

The authors are grateful to journal reviewers, which comments helped to improve the manuscript to a great extent. We appreciate very much the help of Prof. Mark Allen (University of Durham) in discussing the MS and English editing. Dr. Dmitry Ruban (Rostov-na-Donu University) is thanked for helpful ideas and geological literature materials on the Don area. Inna Safonova expresses her cordial thanks to the staff of Titech, especially to Dr. Thuyoshi Komiya, Dr. Shinji Yamamoto, Ms. Shio Watanabe and Mr. Takaaki Nakama, for their help during her stay and work in Tokyo, and to Prof. Mikhail Buslov (IGM SB RAS) for encouraging this research and providing administrative assistance.

Appendix A. Supplementary data

Supplementary data associated with this article can be found, in the online version, at doi:10.1016/j.jog.2010.02.008.

References

Abbott, D.H., Isley, A.E., 2002. The intensity, occurrence, and duration of superplume events and eras over geological time. Journal of Geodynamics 34, 265–307.

Aftalion, M., Bibikova, E.V., Bowes, D.R., Hopgood, A.M., Perchuk, L.L., 1991. Timing of early proterozoic collisional and extensional events in the granulite-gneiss-charnokite-granite complex, Lake Baikal, USSR: a U–Pb, Rb–Sr, and Sm–Nd isotopic study. Journal of Geology 99, 851–862.

Alekseev, A.A., 1984. Riphean-Vendian Magmatism of the Western Slope of the Urals. Nauka, Moscow (in Russian).

Allen, M.B., Morton, A., Fanning, C., Ismail-Zadeh, A.J., Kroonenberg, A., 2006. Zircon age constraints on sediment provenance in the Caspian region. Journal of the Geological Society, London 163, 647–655.

Armstrong, R.L., 1991. The persistent myth of crustal growth. Australian Journal of Earth Sciences 38, 613–630.

Bea, F., Fershtater, G., Montero, P., Smirnov, V., Molina, J., 2005. Deformation driven differentiation of granite magma: the Stepninsk pluton of the Uralides, Russia. Lithos 81, 209–233.

Badarch, G., Cunningham, W.D., Windley, B.F., 2002. A new terrane subdivision for Mongolia: implications for the Phanerozoic crustal growth of Central Asia. Journal of Asian Earth Sciences 21, 87–110.

Bibikova, E.V., Williams, I.S., 1990. Ion-microprobe U–Th–Pb isotopic studies of zircons from three early Precambrian areas in the USSR. Precambrian Research 48, 2–3–221.

Bogdanova, S.V., 1986. Earth Crust of the Russian Platform in the Early Precambrian (the Volga-Ural region as example). Nauka, Moscow (in Russian).

Bogdanova, S., 1993. Segments of the east European craton. In: Gee, D.G., Beckholmen, M. (Eds.), EUROPROBE in Jablonna 1991. Institute of Geophysics, Polish Academy of Sciences-European Science Foundation, Warsaw.

Bogdanova, S.V., Bingen, B., Gorbatschev, R., Kheraskova, T.N., Kozlov, V.I., Puchkov, V.N., Volozh, Yu A., 2008. The East European Craton (Baltica) before and during the assembly of Rodinia. Precambrian Research 160, 23–45.

Buslov, M.M., Safonova, I.Yu., Watanabe, T., Obut, O., Fujiwara, Y., Iwata, K., Semakov, N.N., Sugai, Y., Smirnova, L.V., Kazansky, A.Yu., 2001. Evolution of the Paleo-Asian Ocean (Altai-Sayan region, Central Asia) and collision of possible Gondwana-derived terranes with the southern marginal part of the Siberian continent. Geosciences Journal 5, 203–224.

Buslov, M.M., Fujiwara, Y., Iwata, K., Semakov, N.N., 2004a. Late Paleozoic-Early Mesozoic geodynamics of Central Asia. Gondwana Research 7, 791–808.

Buslov, M.M., Watanabe, T., Fujiwara, Y., Iwata, K., Smirnova, L.V., Safonova, I.Yu., Semakov, N.N., Kiryanova, A.P., 2004b. Late Paleozoic faults of the Altai region, Central Asia: tectonic pattern and model of formation. Journal of Asian Earth Sciences 23, 655–671.

Buslov, M.M., Safonova, I.Yu., Fedoseev, G.S., Reichow, M., Travin, A.V., Babin, G.A., 2007. Plume-related basalts of the Kuznetsk Basin. In: Seltmann, R., Borisenko, A., Fedoseev, G. (Eds.), Magmatism and Metallogeny of the Altai and Adjacent Large Igneous Provinces with an Introductory Essay on the Altaids, IAGOD Guidebook Series 16. CERCAMS/NHM, London, pp. 121–135.

Cawood, P.A., Nemchin, A.A., Freeman, M., Sircombe, K., 2003. Linking source and sedimentary basin: detrital zircon record of sediment flux along a modern river system and implications for provenance studies. Earth and Planetary Science Letters 210, 259–268.

Claoue-Long, J.C., Sobolev, N.V., Shatsky, V.S., Sobolev, A.V., 1991. Zircon response to diamond-pressure metamorphism in the Kokchetav massif, USSR. Geology 19, 710–713.

Cocks, L.M., Torsvik, T.H., 2007. Siberia, the wondering northern terrane, and its changing geography through the Paleozoic. Earth-Science Reviews 82, 29–74.

Collins, A.S., Pisarevsky, S.A., 2005. Amalgamating eastern Gondwana: the evolution of the Circum-Indian orogens. Earth-Science Reviews 71, 229–270.

Condie, K.C., 1998. Episodic continental growth and supercontinents: a mantle avalanche connection? Earth and Planetary Science Letters 163, 97–108.

Condie, K.C., 2000. Episodic continental growth models: afterthoughts and extensions. Tectonophysics 322, 153–162.

Condie, K.C., 2001. Rodinia and continental growth. Gondwana Research 4, 154–155.

Condie, K.C., 2002. Continental growth during a 1.9-Ga superplume event. Journal of Geodynamics 34, 249–264.

Condie, K.C., 2005. Breakup of a Paleoproterozoic supercontinent. Gondwana Research 5, 41–43.

Condie, K.C., Belousova, E., Griffin, W.L., Sircombe, K.N., 2009. Granitoid events in space and time: constraints from igneous and detrital zircon age spectra. Gondwana Research 15, 228–242.

Deer, W.A., Howie, R.A., Zussman, J., 1997. Rock-forming Minerals, vol. 1A: Orthosilicates, 2nd ed. Geological Society, London.

Dewey, J.F., Windley, B.F., 1981. Growth and differentiation of continental crust. Philosophical Transaction of the Royal Society of London, A 301, 189–206.

Didenko, A.N., Mossakovskiy, A.A., Pecherskiy, D.M., Ruzhentsev, S.G., Samygin, S.G., Kheraskova, T.N., 1994. Geodynamics of Paleozoic oceans of Central Asia. Russian Geology and Geophysics 35, 48–62.

Dobretsov, N.L., Buslov, M.M., 2007. Late Cambrian-Ordovician tectonics and geodynamics of Central Asia. Russian Geology and Geophysics 48, 1–12.

Dobretsov, N.L., Berzin, N.A., Buslov, M.M., 1995. Opening and tectonic evolution of the Paleo-Asian Ocean. International Geology Review 37, 335–360.

Eggins, S.M., Rudnick, R.L., McDonough, W.F., 1998. The composition of peridotites and their minerals: a laser-ablation ICP–MS study. Earth and Planetary Science Letters 154, 53–71.

Fershtater, G.B., Montero, P., Borodina, N.S., Pushkarev, E.V., Smirnov, V.N., Bea, F., 1997. Uralian magmatism: an overview. Tectonophysics 297, 87–102.

Fershtater, G.B., Krasnobaev, A.A., Bea, F., Montero, P., Levin, V.Ya., Kholodnov, V.V., 2009. Isotopic-geochemical features and age of zircons in dunites of the platinum-bearing type Uralian massifs: petrogenetic implications. Petrology 17, 503–520.

Gladkochub, D.P., Pisarevsky, S.A., Donskaya, T.V., Natapov, L.M., Mazukabzov, A.M., Stanevich, A., Sklyarov, E.V., 2006. The Siberian Craton and its evolution in terms of the Rodinia hypothesis. Episodes 29, 169–174.

Gladkochub, D.P., Pisarevsky, S.A., Donskaya, T.V., Ernst, R.E., Wingate, M.T., Soderlung, U., Mazukabzov, A.M., Sklyarov, E.V., Hamilton, M.A., Hanes, J.A., 2010. Proterozoic mafic magmatism in Siberian craton: An overview and implications for paleocontinental reconstruction. Precambrian Research doi:10.1016/j.precamres.2010.02.023.

Glasmacher, U.A., Bauer, W., Giese, U., Reynolds, P., Kober, B., Puchkov, V., Stroink, L., Alekseyev, A., Willner, A.P., 2001. The metamorphic complex of Beloretzk, SW Urals, Russia—a terrane with a polyphase Meso to Neoproterozoic thermodynamic evolution. Precambrian Research 110, 185–213.

Guinn, J., 2006. Comparison of Detrital Zircon Age Distributions Using the K–S Test. University of Arizona, Tucson.

Heinhorst, J., Lehmann, B., Ermolov, P., Serykh, V., Zhurutin, S., 2000. Paleozoic crustal growth and metallogeny of Central Asia: evidence from magmatic-hydrothermal ore systems of Central Kazakhstan. Tectonophysics 328, 69–87.

Hermann, J., Rubatto, D., Korsakov, A.V., Shatsky, V.S., 2006. The age of metamorphism of diamondiferous rocks determined with SHRIMP dating of zircon. Russian Geology and Geophysics 47, 511–518.

Hirata, T., Nesbitt, R.W., 1995. U–Pb isotope geochronology of zircon: evaluation of the laser probe-inductively coupled plasma mass spectrometry technique. Geochimica et Cosmochimica Acta 59, 2491–2500.

Hirata, T., Iizuka, T., Orihashi, Y., 2005. Reduction of mercury background on ICP-mass spectrometry for in-situ U–Pb age determinations of zircon samples. Journal of Analytical Atomic Spectrometry 20, 696–701.

Hirata, T., 2000. Development of a flushing spray chamber for inductively coupled plasma-mass spectrometry. Journal of Analytical Atomic Spectrometry 15, 1447–1450.

Hoffman, P.F., 1991. Did the breakout of Laurentia turn Gondwanaland inside out? Science 252, 1409–1412.

Hong, D., Zhang, J., Wang, T., Wang, Sh., Xie, X., 2004. Continental crust growth and the supercontinental cycle: evidence from the Central Asian orogenic belt. Journal of Asian Earth Sciences 23, 799–813.

Hoskin, P.W.O., Black, L.P., 2000. Metamorphic zircon formation by solid-state recrystallization of protolith igneous zircon. Journal of Metamorphic Geology 18, 423–439.

Jahn, B., Wu, F., Chen, B., 2000. Granitoids of the Central Asian Orogenic Belt and continental growth in the Phanerozoic. Transactions of the Royal Society of Edinburgh 91, 181–193.

Jahn, B., 2004. Phanerozoic continental growth in Central Asia. Journal of Asian Earth Sciences 23, 599–603.

Jahn, B., Capdevila, R., Liu, D., Vernon, A., Badarch, G., 2004. Sources of Phanerozoic granitoids in the transect Bayanhongor–Ulaan Baatar, Mongolia: geochemical and Nd isotopic evidence, and implications for Phanerozoic crustal growth. Journal of Asian Earth Sciences 23, 629–653.

Karsakov, L.P., Zhao, Ch., Goroshko, M.V., Roganov, G.V., Varnavsky, V.G., Mishin, L.F., Malyshev, Yu.F., Lu, Z., Gornov, P.Yu., Kaplun, V.B., Manilov, F.I., Podgorny, V.Ya., Romanovsky, N.F., Shevchenko, B.F., Rodionov, S.M., Duan, R., Zhu, Q., Kuznetsov, V.E., Stepahsko, A.A., 2005. Tectonics, deep structure, metallogeny of the Central Asian–Pacific belts junction area. In: Explanatory Notes to the Tectonic Map Scale of 1/1,500,000. FEB RAS, Khabarovsk (in Russian).

Kemp, A.I.S., Hawkesworth, C.J., Paterson, B.A., Kinny, P.D., 2006. Episodic growth of the Gondwana supercontinent from hafnium and oxygen isotopes in zircon. Nature 439, 580–583.

Khain, V.E., Nikishin, A.M., 1998. Russia. In: Moores, E.M., Fairbridge, R.W. (Eds.), Encyclopedia of European and Asian geology. Springer.

Kovalenko, V.I., Yarmolyuk, V.V., Kovach, V.P., Kotov, A.B., Kozakov, I.K., Salnikova, E.B., Larin, A.M., 2004. Isotope provinces, mechanisms of generation and sources of the continental crust in the Central Asian mobile belt: geological and isotopic evidence. Journal of Asian Earth Science 23, 605–627.

Kroner, A., Windley, B., Badarch, G., Tomurtogoo, O., Hegner, E., Jahn, B.M., Gruschka, S., Khain, E.V., Demoux, A., Wingate, M.T.D., 2007. Accretionary growth and crust formation in the Central Asian orogenic belt and comparison with the Arabian-Nubian shield. In: Hatcher Jr., R.D., Carlson, M.P., McBride, J.H., Martinez Catalan, J.R. (Eds.), Framework of Continental Crust, vol. 200. Geological Society of America Memoir, pp. 181–209.

Kruk, N.N., Rudnev, S.N., Vladimirov, A.G., Zhuravlev, D.Z., 1999. Sm-Nd isotopic system of the granitoids in western Altay-Sayan folded area. Doklady Earth Sciences 366 (4), 569–575.

Letnikov, F.A., Watanabe, T., Kotov, A.B., Yokoyama, K., Zyryanov, A.S., Kovach, V.P., Gladkochub, D.P., 2001. Problem of the Age of Metamorphic Rocks of the Kokchetav Block, Northern Kazakhstan. Doklady Earth Sciences 381A, 1025–1027.

Li, Z.X., Bogdanova, S.V., Collins, A.S., Davidson, A., De Waele, B., Ernst, R.E., Fitzsimons, I.C.W., Fuck, R.A., Gladkochub, D.P., Jacobs, J., Karlstrom, K.E., Lu, S., Natapov, L.M., Pease, V., Pisarevsky, S.A., Thrane, K., Vernikovsky, V., 2008. Assembly, configuration, and break-up history of Rodinia: a synthesis. Precambrian Research 160, 179–210.

Ludwig, K.R., 1999. Isoplot, a Geochronological Toolkit for Microsoft Excel. Berkeley Geochronology Center Special Publication No. 1a.

Maruyama, S., Santosh, M., Zhao, D., 2007. Superplume, supercontinent and post-perovskite: mantle dynamics and anti-plate tectonics on the Core–Mantle boundary. Gondwana Research 11, 7–37.

Maruyama, Sh., Isozaki, Yu., Kimura, G., Terabayashi, M., 1997. Paleogeographic maps of the Japanese Islands: plate tectonic synthesis from 750 Ma to the present. Island Arc 6, 121–142.

Maystrenko, Yu., Stovba, S., Stephenson, R., Bayer, U., Menyoli, E., Gajewski, D., Huebscher, Ch., Rabbel, W., Saintot, A., Starostenko, V., Thybo, H., Tolkunov, A., 2003. Crustal-scale pop-up structure in cratonic lithosphere: DOBRE deep seismic reflection study of the Donbas fold belt, Ukraine. Geology 31, 733–736.

McCulloch, M.T., Bennet, V.C., 1994. Progressive growth of the Earth's continental crust and depleted mantle: geochemical constrains. Geochimica et Cosmochimica Acta 58, 4717–4738.

McMenamin, M.A.S., McMenamin, D.I.S., 1990. The Emergence of Animals: The Cambrian Breakthrough. Columbia University Press, New York.

Meert, J.G., Lieberman, 2008. The Neoproterozoic assembly of Gondwana and its relationship to the Ediacaran–Cambrian radiation. Gondwana Research 14, 5–21.

Milanovsky, E.E., Nikishin, A.M., Furne, A.V., 1994. Riphean history of the East European Craton. Doklady Rossiiskoi Akademii Nauk 339, 513–517 (in Russian).

Molnar, P., Tapponnier, P., 1975. Cenozoic tectonics of Asia: effects of a continental collision. Science 189, 419–426.

Murphy, J.B., Nance, R.D., Cawood, A., 2009. Contrasting modes of supercontinent formation and the conundrum of Pangea. Gondwana Research 15, 408–420.

Nalivkin, D.V., 1983. Geological Map of the USSR and Adjacent Water-covered Areas. Ministry of Geology of the USSR, Moscow.

Necheukhin, V.M., Krasnobaev, A.A., Sokolova, V.B., 2000. Ancient continental crust terranes in accretion-collisional structures of the Urals. Doklady Earth Sciences 370, 655–657.

Nikishin, A.M., Ziegler, P.A., Stephenson, R.A., Cloetingh, S.A.P.L., Fume, A.V., Fokin, P.A., Ershov, A.V., Bolotov, S.N., Korotaev, M.V., Alekseev, A.S., Gorbachev, V.I., Shipilov, E.V., Lankreijer, A., Bembinova, E.Yu., Shalimov, I.V., 1996. Late Precambrian to Triassic history of the East European Craton: dynamics of sedimentary basin evolution. Tectonophysics 268, 23–63.

Nozhkin, A.D., Turkina, O.M., Bibikova, E.V., Terleev, A.A., Khomentovsky, V.V., 1999. Riphean granite-gneiss domes of the Yenisey Ridge: geological structure and U–Pb isotopic age. Russian Geology and Geophysics 40, 1284–1293.

Parfenov, L.M., Khanchuk, A.I., Badarch, G., Miller, R.J., Naumova, V.V., Nokleberg, W.J., Ogasawara, M., Prokopiev, A.V., Yan, H., 2006. North-East Asia Geodynamic Map., http://pubs.usgs.gov/of/2006/geopubs.wr.usgs.gov/open-file/of03-205/.

Press, W.H., Flannery, B.P., Teukolsky, S.A., Vetterling, W.T., 1986. Numerical Recipes: The Art of Scientific Computing. Cambridge University Press, Cambridge.

Prokopiev, A., Toro, J., Miller, E.L., Gehrels, G.E., 2008. The paleo–Lena River—200 m.y. of transcontinental zircon transport in Siberia. Geology 36, 699–702.

Puchkov, V.N., 1997. Structure and geodynamics of the Uralian orogen. In: Burg, J.-P., Ford, M. (Eds.), Orogeny Through Time, 121. Special Publications, Geological Society, London, pp. 201–236.

Puchkov, V.N., 2003. Uralides and Timanides; their structural relationship and position in the geologic history of the Ural-Mongolian foldbelt. Russian Geology and Geophysics 44, 27–38.

Rey, P.F., Philippot, P., Thebaud, N., 2003. Contribution of mantle plumes, crustal thickening and greenstone blanketing to the 2.75–2.65 Ga global crisis. Precambrian Research 127, 43–60.

Reymer, A., Schubert, G., 1984. Phanerozoic addition rates to the continental crust and crustal growth. Tectonics 3, 63–77.

Rino, Sh., Komiya, T., Windley, B., Katayama, I., Motoki, A., Hirata, T., 2004. Major episodic increases of continental crustal growth determined from zircon ages of river sands: implications for mantle overturns in the Early Precambrian. Physics of Earth and Planetary Interiors 146, 369–394.

Rino, S., Kon, Y., Sato, W., Maruyama, S., Santosh, M., Zhao, D., 2008. The Grenvillian and Pan-African orogens: world's largest orogenies through geologic time, and their implications on the origin of superplume. Gondwana Research 14, 51–72.

Rogers, J.J.W., Santosh, M., 2002. Configuration of Columbia, a Mesoproterozoic supercontinent. Gondwana Research 5, 5–22.

Rogers, J.J.W., Santosh, M., 2003. Supercontinents in earth history. Gondwana Research 6, 357–368.

Rogers, J.J.W., Santosh, M., 2009. Tectonics and surface effects of the supercontinent Columbia. Gondwana Research 15, 373–380.

Rosen, O.M., Nozhkin, A.D., Condie, K.C., 1993. Active margin of the Tungus protocontinent in the early Proterozoic: the earliest shoreline of the Paleo-Asian Ocean? In: Dobretsov, N.L., Berzin, N.A. (Eds.), Proceedings of the 4th International Symposium on Dynamic evolution of the Paleo-Asian Ocean. UIGGM, Novosibirsk.

Rosen, O.M., Condie, K.C., Natapov, L.M., Nozhkin, A.D., 1994. Archean and Early Proterozoic evolution of the Siberian craton: a preliminary assessment. In: Condie, K.C. (Ed.), Archean Crustal Evolution. Elsevier, Amsterdam.

Ruban, D.A., Yoshioka, S., 2005. Late Paleozoic-Early Mesozoic Tectonic Activity Within the Donbass (Russian Platform).

Safonova, I., Rino, S., Maruyama, S., Buslov, M., Kon, Y., 2009a. Rodinia and Gondwana derived microcontinents in the bedrock of the Ob' River basin, West Siberia: evidence from the U–Pb dating of detrital zircons. In: The 2009 IAGR Annual Convention and 6th International Symposium on Gondwana to Asia, Hanoi, Vietnam, October 2–6, 2009, pp. 15–16 (Abstracts).

Safonova, I.Yu., Utsunomiya, A., Kojima, S., Nakae, S., Koizumi, K., Tomurtogoo, O., Filippov, A.N., 2009b. Pacific superplume-related oceanic basalts hosted by accretionary complexes of Central Asia, Russian Far East and Japan. Gondwana Research 16, 587–608.

Safonova, I.Yu., Rino, S., Maruyama, S., 2010. U–Pb age of detrital zircons from modern sediments of the Yangtze River and stages of orogeny in South-East Asia. Doklady Earth Sciences 431 (1), 280–284.

Sakhno, V.G., 2001. Late Mesozoic and Cenozoic Continental Volcanism of East Asia. Dalnauka, Vladivostok (in Russian).

Samsonov, A.V., Chernyshev, I.V., Nutman, A.P., Compston, W., 1996. Evolution of the Archaean Aulian Gneiss Complex, Middle Dnieper gneiss–greenstone terrain, Ukrainian Shield: SHRIMP U–Pb zircon evidence. Precambrian Research 78, 65–78.

Samygin, S.G., Burtman, V.S., 2009. Tectonics of the Ural Paleozoids in comparison with the Tien Shan. Geotectonics 2, 57–77 (in Russian with English abstract).

Santosh, M., Maruyama, S., Yamamoto, S., 2009. The making and breaking of supercontinents: some speculations based on superplumes, super downwelling and the role of tectosphere. Gondwana Research 15, 324–341.

Scotese, C.R., 2004. A continental drift flipbook. Journal of Geology 11, 729–741.

Sengör, A.M.C., Natal'in, B.A., Burtman, V.S., 1993. Evolution of the Altaid tectonic collage and Palaeozoic crustal growth in Eurasia. Nature 364, 299–307.

Shatsky, V.S., Sobolev, N.V., Vavilov, M.A., 1995. Diamond bearing metamorphic rocks of the Kokchetav Massif (northern Kazakhstan). In: Coleman, R.G., Wang, X. (Eds.), Ultrahigh-Pressure Metamorphism. Cambridge Univ. Press, Cambridge, pp. 427–455.

Shchipansky, A.A., Bogdanova, S.V., 1996. The Sarmatian crustal segment: Precambrian correlation between the Voronezh Massif and the Ukrainian Shield across the Dniepr–Donets Aulacogen. Tectonophysics 268, 109–125.

Shchipansky, A.A., Samsonov, A.V., Petrova, A. Yu., Larionova, Yu. O., 2007. Geodynamics of the Eastern margin of Sarmatia in the Paleoproterozoic. Geotectonics 1, 43–70.

Smelov, A., Timofeev, V.F., 2007. The age of the North Asian Cratonic basement: an overview. Gondwana Research 12, 279–288.

Stampfli, G.M., Borel, G.D., 2002. A plate tectonic model for the Paleozoic and Mesozoic constrained by dynamics plate boundaries and restored synthetic oceanic isochrones. Earth and Planetary Science Letters 196, 17–33.

Stein, M., Hofmann, A.W., 1994. Mantle plumes and episodic crustal growth. Nature 372, 63–68.

Stern, R.G., 2008. Neoproterozoic crustal growth: the solid earth system during a critical episodic of earth history. Gondwana Research 14, 33–50.

Turkina, O.M., Noshkin, A.D., Bayanova, T.B., 2007. Sources and formation conditions of early proterozoic granitoids from the southwestern margin of the Siberian Craton. Petrology 14, 282–303.

Vernikovsky, V.A., Vernikovskaya, A.E., 2006. Tectonics and evolution of granitoid magmatism in the Yenisei Ridge. Russian Geology and Geophysics 47, 32–50.

Vladimirov, A.G., Ponomareva, A.P., Shokalsky, S.P., Khalilov, V.A., Kostitsyn, Yu.A., Ponomarchuk, V.A., Rudnev, S.N., Vystavnoi, S.A., Kruk, N.N., Titov, A.V., 1997. Late Paleozoic-Early Mesozoic granitoid magmatism in Altay. Russian Geology and Geophysics 38, 755–771.

Vladimirov, A.G., Vystavnoi, S.A., Titov, A.V., Rudnev, S.N., Dergachev, V.B., Annikov, I. Yu., Tikunov, Yu. V., 1998. Petrology of the Early Mesozoic rare-metal granites of the southern Gorny Altay. Russian Geology and Geophysics 39, 909–925.

Vladimirov, A.G., Ponomareva, A.P., Kargopolov, S.A., Babin, G.A., Plotnikov, A.V., Gibsher, A.S., Izokh, A.E., Shokalsky, S.P., Bibikova, E.V., Zhuravlev, D.Z., Ponomarchuk, V.A., Khalilov, V.A., Travin, A.V., 1999. Neoproterozoic age of the oldest rocks in the Tom' Uplift, Gornaya Shoriya based on U–Pb, Sm-Nd and Ar-Ar isotopic dating. Stratigraphy. Geological Correlation 7, 28–42 (in Russian).

Weislogel, A.L., Graham, S.A., Chang, E.Z., Wooden, J.L., Gehrels, G.E., Yang, H.S., 2006. Detrital zircon provenance of the Late Triassic Songpan-Ganzi complex: sedimentary record of collision of the North and South China blocks. Geology 34, 97–100.

Whitehouse, M.J., Kamber, B.S., Moorbath, S., 1999. Age significance of U–Th–Pb zircon data from Early Archean rocks of west Greenland—a reassessment based on combined ion-microprobe and imaging studies. Chemical Geology 160, 201–224.

Williams, H., Hoffman, P.F., Lewry, J.F., Monger, J.W.H., Rivers, T., 1991. Anatomy of North America: thematic portrayals of the continent. Tectonophysics 187, 117–134.

Wilson, M., Lyashkevich, Z.M., 1996. Magmatism and the geodynamics of rifting of the Pripyat-Dnieper-Donets rift, East European platform. Tectonophysics 268, 65–81.

Windley, B.F., Kroner, A., Guo, J., Qu, G., Li, Y., Zhang, Ch., 2002. Neoproterozoic and Paleozoic geology of the Altai orogen, NW China: new zircon age data and tectonic evolution. Journal of Geology 110, 719–737.

Yarmolyuk, V.V., Litvinovsky, B.A., Kovalenko, V.I., Jahn, B.M., Zanvilevich, A.N., Vorontsov, A.A., Zhuravlev, D.Z., Posokhov, V.F., Kuzmin, D.V., Sandimirova, G.P., 2001. Formation stages and sources of the peralkaline granitoid magmatism of the Northern Mongolia-Transbaikalia Rift Belt during the Permian and Triassic. Petrology 9, 302–328.

Yarmolyuk, V.V., Kovalenko, V.I., 2003. Batholiths and geodynamics of batholith formation in the Central Asian fold belt. Russian Geology and Geophysics 44, 1305–1320.

Zonenshain, L.P., Kuzmin, M.I., Natapov, L.M., 1990. Geology of the USSR: a Plate-Tectonic Synthesis. American Geophysical Union. Geodynamic Series 21.